Development 129, 2591-2606 (2002)
Printed in Great Britain © The Company of Biologists Limited 2002
DEV5932

The *jing* Zn-finger transcription factor is a mediator of cellular differentiation in the *Drosophila* CNS midline and trachea

Yalda Sedaghat*, Wilson F. Miranda* and Margaret J. Sonnenfeld†

Department of Cellular and Molecular Medicine, Faculty of Medicine, University of Ottawa, Ottawa, Ontario K1H 8M5, Canada
*These authors contributed equally to this work
†Author for correspondence (e-mail: msonnenf@uottawa.ca)

Accepted 2 March 2002

SUMMARY

We establish that the *jing* zinc-finger transcription factor plays an essential role in controlling CNS midline and tracheal cell differentiation. *jing* transcripts and protein accumulate from stage 9 in the CNS midline, trachea and in segmental ectodermal stripes. JING protein localizes to the nuclei of CNS midline and tracheal cells implying a regulatory role during their development. Loss of *jing-lacZ* expression in homozygous *sim* mutants and induction of *jing-lacZ* by ectopic *sim* expression establish that *jing* is part of the CNS midline lineage. We have isolated embryonic recessive lethal *jing* mutations that display genetic interactions in the embryonic CNS midline and trachea, with mutations in the bHLH-PAS genes *single-minded* and *trachealess*, and their downstream target genes (*slit* and *breathless*). Loss- and gain-of-function *jing* is associated with defects in CNS axon and tracheal tubule patterning. In *jing* homozygous mutant embryos, reductions in marker gene expression and inappropriate apoptosis in the CNS midline and trachea establish that *jing* is essential for the proper differentiation and survival of these lineages. These results establish that *jing* is a key component of CNS midline and tracheal cell development. Given the similarities between JING and the vertebrate CCAAT-binding protein AEBP2, we propose that *jing* regulates transcriptional mechanisms in *Drosophila* embryos and promotes cellular differentiation in ectodermal derivatives.

Key words: *jing*, Zinc finger, CNS midline, Trachea, *Drosophila*

INTRODUCTION

Transcriptional regulatory mechanisms play an important role in cell fate determination in both vertebrates and invertebrates. Transcription factors have multiple roles in controlling cellular competence or determination and also in regulating differentiation (Cau et al., 2000; Hallam et al., 2000; Moran-Rivard et al., 2001; Pierani et al., 2001; Portman and Emmons, 2000). The combinatorial nature of transcriptional regulation during cellular specification is emerging from studies of diverse embryonic tissues including the nervous system and respiratory system (trachea) (Boube et al., 2000; Jurata et al., 2000; Ma et al., 2000; Zelzer and Shilo, 2000). In addition, different categories of transcription factors can function at successive steps during cellular development. In this way, cellular responses may be dictated by the temporal and spatial characteristics of multiple and/or diverse types of transcription factors.

In *Drosophila*, the ventral midline and respiratory system (trachea) are ectodermal derivatives patterned by positional cues present in embryos. The ventral midline is patterned by the combinatorial actions of dorsal/ventral (D/V) and neurogenic genes that confine the expression of the bHLH-PAS transcription factor *single-minded* (*sim*) to the mesectoderm (Crews, 1998; Morel and Schweisguth, 2000). Development of the entire CNS midline requires the regulatory functions of *sim* and in the absence of *sim* function midline cells take on lateral neuroectodermal fates (Crews, 1998; Estes et al., 2001; Nambu et al., 1991; Xiao et al., 1996). The midline-inducing capabilities of *sim* were discovered by ectopic expression experiments (Nambu et al., 1991). Subsequent CNS midline gene regulation involves the combinatorial functions of three different transcription factors including bHLH-PAS, SOX and POU domain-containing proteins (Ma et al., 2000). CNS midline precursors give rise to midline glia and various interneuron and motoneuron lineages including two MP1 neurons, two UMI neurons, the MNB and VUMs (Klämbt et al., 1991; Bossing and Technau, 1994; Schmid et al., 1999).

The tracheal placodes are specified by TGFβ signaling along the dorsoventral axis and Wingless (WG) signaling along the anteroposterior axis (Affolter et al., 1994; de Celis et al., 1995; Wilk et al., 1996). These cues are responsible for independently activating primary genes such as the bHLH-PAS transcription factor *trachealess* (*trh)* and the POU domain transcription factor *ventral veinless* (*vvl*) (previously known as *drifter*), which are required in a combinatorial fashion for subsequent tracheal development (Boube et al., 2000; Isaac and Andrew, 1996; Llimargas and Casanova, 1997; Wilk et al.,

1996; Zelzer and Shilo, 2000). In the absence of *trh* and *vvl* function tracheal cells fail to invaginate and tracheal tubules do not form (de Celis et al., 1995; Isaac and Andrew, 1996; Wilk et al., 1996). Ectopic *trh* expression can induce tracheal pits and therefore it has been considered an inducer of cell fates (Wilk et al., 1996). Within the trachea, the DPP pathway specifies the fates of branches that will give rise to the dorsal branch and lateral anterior and posterior branches (Affolter et al., 1994; Vincent et al., 1997; Wappner et al., 1997). Activation of the EGF receptor pathway is required for specifying the dorsal trunk and visceral branch (Wappner et al., 1997). In addition, the WNT pathway is required for specification of the dorsal trunk (Llimargas, 2000; Chihara and Hayashi, 2000).

The invertebrate ortholog of the aryl hydrocarbon nuclear translocator, known as *tango* (*tgo*), encodes a common partner for SIM and TRH (Oshiro and Saigo, 1997; Sonnenfeld et al., 1997; Zelzer et al., 1997). TGO is present in the cytoplasm and translocates to the nucleus upon expression of a dimerization partner such as *sim*, *trh* or *Spineless-Aristapedia* (*ss*) (Emmons et al., 1999; Ward et al., 1998). Therefore, the precise regulation of lineage-specific transcriptional regulators such as *sim*, *trh* and *ss* is critical. In both the CNS midline and trachea, TGO::SIM and TGO::TRH heterodimers activate common target genes containing asymmetrical E-box sites with an ACGTG core (Crews, 1998; Zelzer and Shilo, 2000). These E-box sequences are sufficient to drive both midline and tracheal expression and are required for the expression of known target genes including the *breathless* fibroblast growth factor receptor and the repulsive guidance molecule *slit* (Battye et al., 1999; Glazer and Shilo, 1991; Kidd et al., 1999; Sonnenfeld et al., 1997; Wharton et al., 1994).

In this study, we have used genetic and cellular analysis to establish novel roles for the *jing* zinc-finger transcription factor in the differentiation of CNS midline and tracheal cells. A genetic approach to identify molecules required for the commitment of CNS midline and tracheal cells led to the identification and characterization of the *jing* locus during embryogenesis. The *jing* locus has been previously identified in genetic screens and recently characterized for its role in border cell migration in *Drosophila* ovaries (Karpen and Spradling, 1992; Liu and Montell, 2001). During embryogenesis, *jing* transcripts and protein are detected in the CNS midline, trachea and segmental ectodermal stripes. Gene dosage and overexpression experiments reveal that appropriate levels of *jing* in the CNS midline and trachea are crucial for formation of CNS commissural and longitudinal axons as well as tracheal tubules, respectively. Loss-of-function mutations in *jing* are associated with reductions in cell-type gene expression and inappropriate apoptosis of CNS midline and tracheal precursors. These results therefore establish that *jing* is required in a positive manner to promote cellular differentiation and survival in embryonic ectodermal lineages.

MATERIALS AND METHODS

Drosophila strains and genetics

The wild-type strain was w^{118}. The *tango*^{1} (*tgo*^{1}) allele and the *tgo*^{1}*trh*^{8} double mutant strain have been previously described (Sonnenfeld et al., 1997). Double mutant stocks were generated by standard genetic procedures using P element *jing* alleles and null alleles of *single-minded* (*sim*^{H9}) and *trachealess* (*trh*^{1}) (Isaac and Andrew, 1996; Nambu et al., 1990). The second and third balancer chromosomes in these stocks carried the *lacZ*-markers *CyO*P[*wg-lacZ*] and TM3P[*ubx-lacZ*]. The *slit* (*sli*) reporter P[*sli* 1.0 HV-*lacZ*] was used to assess transcription of the *sli* gene (Ma et al., 2000; Wharton et al., 1994). The *breathless*$^{H82\Delta3}$ P-element excision allele (Klämbt et al., 1992) and the null *sli*^{1} allele (Nüsslein-Volhard et al., 1984; Rothberg et al., 1990) were used to assess genetic interactions with multiple *jing* alleles.

P-element lethal stocks were obtained from the Indiana University *Drosophila* Stock Center (Bloomington, Indiana). The *jing-lacZ* enhancer trap strain (*jing*^{01094}) contains an embryonic recessive lethal insertion of the P-element P[PZ] originally designated l(2)*01094* (BDGP) (Karpen and Spradling, 1992; Spradling et al., 1999). l(2)*01094*^{K03404} is a second embryonic lethal insertion of the P[*lacW*] P-element in the *jing* gene (from I. Kiss, T. Laverty and G. Rubin) (Liu and Montell, 2001) and we refer to this allele as *jing*^{K03404}. Both alleles do not complement the lethality of a *jing* deficiency Df(2R)ST1 (Liu and Montell, 2001).

The P[*sim*-UAS] and P[*prd*-Gal4] strains were used to ectopically express *sim* under control of a *prd* enhancer in a background heterozygous for the *jing-lacZ* enhancer trap (Brand and Perrimon, 1993; Ward et al., 1998; Xiao et al., 1996). P[*sim*-GAL4] and P[*btl*-GAL4] were used as drivers to overexpress *jing* in the CNS midline and trachea, respectively (Shiga et al., 1996; Ward et al., 1998).

Molecular analysis of *jing*, P[UAS-*jing*] construction and antibody production

Genomic DNA surrounding the P element insertions in *jing*^{01094} and *jing*^{K03404}flies, and including *jing*-coding sequences, was sequenced and deposited into GenBank (AF285778). Expressed sequence tags (ESTs) LD10015, LD36562 and LD10101 were identified by database searching, obtained from Research Genetics (Birmingham, AL) and subjected to DNA sequence analysis. Gel-purified fragments of PCR-generated genomic and EST DNA were sequenced on both strands by dye terminator cycle DNA sequencing (Perkin Elmer) using an ABI PRISM Genetic Analyzer. LD36562 and LD10101 sequences were identical to FlyBase Genome Annotation Database (GadFly) identifier CG9403 (http://flybase.bio.indiana.edu/annotl) (Adams et al., 2000).

The *jing* full-length cDNA (LD36562) was cloned into pUAST (Brand and Perrimon, 1993) and together with pUChspΔ2,3 P element helper plasmid was injected into *y w* embryos and w^{+} transformants were selected (Spradling, 1986). Three transgenic UAS-*jing* lines produced similar results in overexpression experiments using P[*sim*-GAL4] and P[*btl*-GAL4] as drivers (Shiga et al., 1996; Ward et al., 1998).

For antibody production, the JING peptide VPAASANKNKRTAAG (amino acids 81-95) was synthesized (Eastern Quebec Proteomics Core Facility), coupled to KLH (Sigma) and used to generate anti-JING rat antisera (PRF&L). JING antibody specificity was confirmed by examining embryos homozygous for a deficiency in *jing* (Df(2R)ST1) and after ectopic expression of *jing* (*prd*-GAL4/*jing*-UAS).

Antibodies

The following antibodies were used: rat anti-JING (1:100; this work); mAb anti-β-galactosidase (anti-β-gal) (Promega); rabbit polyclonal anti-β-gal (Promega); rat polyclonals anti-Single-minded (anti-SIM) and anti-Trachealess (anti-TRH) (Sonnenfeld et al., 1997; Ward et al., 1998); anti-Wrapper and mAb 1D4 anti-FASCICLIN II (Noordemeer et al., 1998; Lin et al., 1994) (gifts from C. S. Goodman); mAb anti-Slit (a gift from Spyros Artavanis-Tsakonas); mAb 2A12 (a gift from N. Patel); and rabbit anti-Odd-skipped (ODD) (Skeath and Doe, 1998; Spana et al., 1995) (a gift from Jim Skeath). The following antibodies were obtained from the Developmental Studies Hybridoma Bank: mAb BP102;

22C10/FUTSCH (Fujita et al., 1982; Hummel et al., 2000); and mAb 4D9 anti-Engrailed/Invected (Patel et al., 1989).

Immunohistochemistry, in situ hybridization and TUNEL labeling

Embryo staging was carried out according to Campos-Ortega and Hartenstein (Campos-Ortega and Hartenstein, 1985) and processing for light microscopy was undertaken according to standard protocols (Patel, 1994). JING protein distribution was determined by staining whole-mount embryos with rat anti-JING at 1:100 dilution. Antibody staining was visualized using HRP- or rhodamine-conjugated secondary antibodies (Jackson). Balancer chromosomes carrying *lacZ* for the second (*CyO*P[*wg-lacZ*]) and third chromosomes (*TM3*P[*ubx-lacZ*]) were used to identify homozygous mutant embryos after anti-β-gal staining. HRP-labeled embryos were analyzed by light microscopy using a Zeiss Axioskop.

In situ hybridization was performed on w^{118} whole-mount embryos as described (Tautz and Pfeifle, 1989). DNA probes were generated by random priming using wild-type *Drosophila* genomic DNA (GenBank Accession AF285778) and *jing* cDNA (LD36562) as templates. All probes showed identical expression patterns. *jing* DNA probes were labeled with dig-11-dUTP (Boehringer Mannheim) and their specificity determined by in situ hybridization to embryos carrying the Df(2R)ST1 deficiency. Embryos were analyzed by light microscopy.

jing enhancer trap expression was analyzed after staining heterozygous $jing^{01094}$ embryos with anti-β-gal and a secondary antibody conjugated with FITC or rhodamine at 1/250. TUNEL (TMR red; Roche) staining was carried out according to previous procedures and was double stained with anti-SLI, -TRH or -Odd-skipped (Booth et al., 2000). Fluorescently labeled embryos were mounted in 4% n-propyl gallate to inhibit photobleaching and analyzed on a Zeiss Axiovert 100 TV confocal microscope. Optical sections of 1 μm were recorded in line average mode. All figures were processed using Adobe Photoshop software.

Mutagenesis

An F_2 lethal complementation screen using ethylmethane sulfonate (EMS) was performed as described (Grigliatti, 1986; Sonnenfeld et al., 1997). Three lethal EMS-induced *jing* mutations were tested for genetic complementation inter se and with deficiency Df(2R)ST1 (Lui and Montell, 2001). All mutant chromosomes were balanced over *CyO*P[*wg-lacZ*] marked balancers. The $jing^{3}$ EMS-induced allele was sequenced according to previous procedures (Sonnenfeld et al., 1997). Embryonic lethal and viable excision (reversion) $jing^{01094}$ and $jing^{K03404}$ alleles were obtained by standard procedures (Bellen et al., 1989; Robertson et al., 1988). Lethal and viable excisions were isolated by loss of eye color and by genetic complementation and were mapped by PCR using *jing*-specific primers and DNA sequence analysis.

RESULTS

jing mutations display dominant genetic interactions in the CNS with mutations in *sim*, *tgo* and their target *sli*

Dosage-sensitive genetic interactions between two loci are a good indicator that two gene products are functionally related. We identified the *l(2)01094* gene (BDGP) in a search for P-element-induced mutations displaying severe CNS axon phenotypes in double heterozygous combination with null mutations in *sim*. The *l(2)01094* gene has been previously isolated in genetic screens and recently characterized for its role in border cell migration in *Drosophila* ovaries (Karpen and Spradling, 1992; Liu and Montell, 2001). *l(2)01094* encodes a zinc-finger transcription factor called *jing* and we refer to this P-element-induced allele as $jing^{01094}$ (Liu and Montell, 2001).

To address whether *jing* dosage is important for CNS midline development, *jing* P-element insertion mutant alleles were placed in heterozygous combination with null mutations in genes whose primary effects arise from the CNS midline, including *sim* and *sli* mutations. We also tested hypomorphic *tgo* mutations. CNS axon and midline cell development were assessed in double heterozygous embryos by BP102, anti-SIM or anti-SLI staining (Klämbt et al., 1991; Rothberg et al., 1990; Ward et al., 1998). $jing^{01094}$ alleles perturb CNS axon formation and midline cell development in double heterozygous combination with sim^{H9} (Fig. 1C,I; Fig. 2C), tgo^{1} (Fig. 1E,I), and sli^{1} (Fig. 1I; Fig. 2I,K). For example, 54% of *jing* and *sim* double heterozygotes show improper commissural and longitudinal axon formation (‘stalled axons’). A smaller percentage of $jing^{01094}$ and sim^{H9} double heterozygotes (7.7%) show ‘collapsed axon’ phenotypes similar to those of *sim* or *sli* homozygotes (Fig. 1B,I) (Nambu et al., 1990; Rothberg et al., 1990). The phenotypes of *jing* and *sim* double heterozygotes are insertion dependent as they revert to wild- type after precise excision of the P element in $jing^{01094}$ flies (Fig. 1D,I; not shown).

CNS axon and midline cell development are perturbed in embryos triple heterozygous for *jing*, *sim* and *tgo* (Fig. 1F,I; Fig. 2B,E,G). However, unlike in homozygous *sim* mutants, the midline cells in *jing*, *sim* and *tgo* triple heterozygotes are specified but then fail to differentiate properly, as determined by their displacement from the ventral nerve cord (a feature characteristic of apoptotic cells) and loss of Sim immunoreactivity by stage 15 (Fig. 1B; Fig. 2B,E,G) (Sonnenfeld and Jacobs, 1995). The ventral displacement of the CNS midline cells occurs after reduction of one copy of *jing* and *sim*, suggesting that these effects are specific for the midline (Fig. 2C). Triple heterozygotes also show alterations in repulsive signaling mechanisms. Fasciclin 2-positive longitudinal axons collapse into a single tract along the midline in $jing^{01094}$; tgo^{1} sim^{H9} triple heterozygotes stained with 1D4 monoclonal antibody (Fig. 1G,H) (Van Vactor et al., 1993). These phenotypes are, therefore, similar to those of homozygous mutations in sli^{1}, which affect midline repulsion mechanisms and cause the ventral displacement of midline cells (Sonnenfeld and Jacobs, 1994; Battye et al., 1999; Kidd et al., 1999).

To characterize the relationship between *jing* and CNS midline further, we removed one copy of both *jing* and *sli* and analyzed the development of the CNS axons and midline cells. Reducing one copy of both *jing* and *sli* is associated with collapsed axons (55%), the ventral displacement of SIM^{+} midline cells (38%) and reductions in SLI immunoreactivity (40%) in stage 14 embryonic nerve cords compared with wild type (Fig. 1I; Fig. 2I-K). By comparison, 57% of sim^{H9} and sli^{1} double heterozygotes have collapsed axons (Fig. 1I) and ventrally displaced midline cells (45%; Fig. 2I), which is consistent with the established regulatory role of *sim* (Fig. 2H) (Ma et al., 2000; Wharton et al., 1994). Comparison of SIM and SLI immunoreactivity in *jing* and *sli* double heterozygotes therefore reveals that although midline cells are present in these embryos, they do not adequately express *sli*. In summary, these results imply that *jing* dosage may be important for the regulation of *sli*.

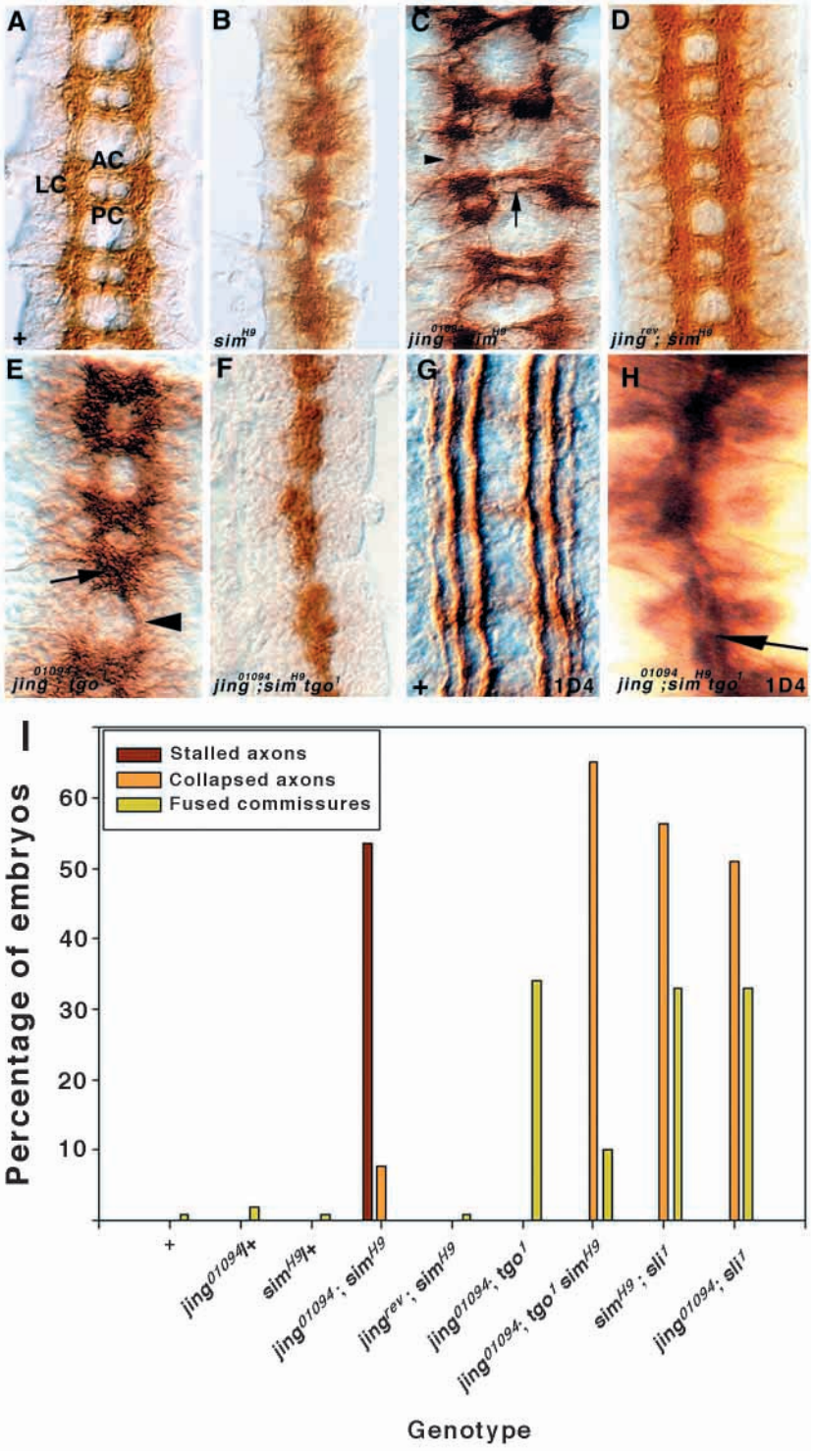

Fig. 1. Genetic interactions in the CNS. (A-F) Preparations of stage 14 ventral nerve cords stained with mAb BP102. Anterior is upwards. (G,H) Stage 15 embryos stained with mAb 1D4 (anti-Fasciclin 2). (A) Wild-type CNS axon scaffold with anterior and posterior commissures (AC and PC) separating longitudinal connectives (LC). (B) Collapsed axon phenotype of a sim^{H9} homozygote. (C) 'Stalled axon' phenotype of $jing^{01094}$; sim^{H9} double heterozygote. Arrow and arrowhead indicate improper commissural and longitudinal formation, respectively. (D) The axon scaffold develops properly in embryos heterozygous for sim^{H9} and a $jing^{01094}$ P element revertant ($jing^{rev}$). (E) The phenotype of embryos heterozygous for tgo^{1} and $jing^{01094}$ resembles weak *sim* phenotypes (arrow) and *spitz* group phenotypes (arrowhead). (F) Severe 'collapsed axon' phenotype in $jing^{01094}$, tgo^{1} sim^{H9} triple heterozygote. (G) Three wild-type 1D4-positive longitudinal fascicles run parallel to the midline. (H) Fusion of longitudinal fascicles in $jing^{01094}$, tgo^{1} sim^{H9} triple heterozygotes. (I) Quantification of *jing* genetic interactions. Double and triple heterozygotes (genotype) were examined for CNS axon scaffold formation using mAb BP102. Data are presented as the percentage of embryos with stalled, collapsed and fused axon phenotypes (n>50 embryos scored in all cases). Note that reduction of one copy of *tgo* in a $jing^{01094}$; *sim* double heterozygote causes a shift in distribution from embryos with stalled axon phenotypes toward those with collapsed axon phenotypes ($jing^{01094}$, tgo^{1} sim^{H9}). $jing^{01094}$ and sim^{H9} mutations show similar dose sensitivities to sli^{1}.

jing mutations interact genetically with mutations in *trh* and its target *breathless*

We next assessed whether *jing* dosage is important for tracheal development by analyzing *jing* in trans-heterozygous combination with mutations in genes whose function is specific for the embryonic trachea. Tracheal tubule development was analyzed in double heterozygous embryos by staining with mAb 2A12, which in wild-type embryos stains the lumen of all tracheal tubules (Fig. 3A). Tracheal tubules do not form in homozygous *trh* mutants (Fig. 3B) (Isaac and Andrew, 1996; Wilk et al., 1996; Sonnenfeld et al., 1997). Tracheal tubule formation is defective after both *trh* and *jing* are reduced by only one copy each. For example, 51% of embryos double heterozygous for $jing^{01094}$ and trh^{1} show a significant loss of most tracheal branches by stage 15 (Fig. 3C,E). In addition, $jing^{01094}$ and trh^{1} double heterozygotes are sensitive to the dose of *tgo*, as 69% of embryos triple heterozygous for these mutations ($jing^{01094}$; trh^{1} tgo^{1}) show tracheal phenotypes (Fig. 3E). *jing* mutations also show dominant interactions with a direct target of TGO and TRH heterodimers, the fibroblast growth factor receptor known as *breathless* (*btl*) (Klämbt et al., 1992; Oshiro and Saigo, 1997). Ninety eight percent of $jing^{01094}$and $btl^{H82\Delta 3}$ double heterozygotes show tracheal phenotypes that affect the formation of transverse connectives and visceral branches (Fig. 3D,E).

In conclusion, the genetic analysis presented here provides strong evidence that proper dose of *jing* in combination with that of *trh* or *btl* is important for tracheal tubule patterning. If *jing* functions in a parallel pathway to that of *trh* and *btl* these results would then indicate that the pathways must converge on a common component that is necessary for tracheal tubule formation.

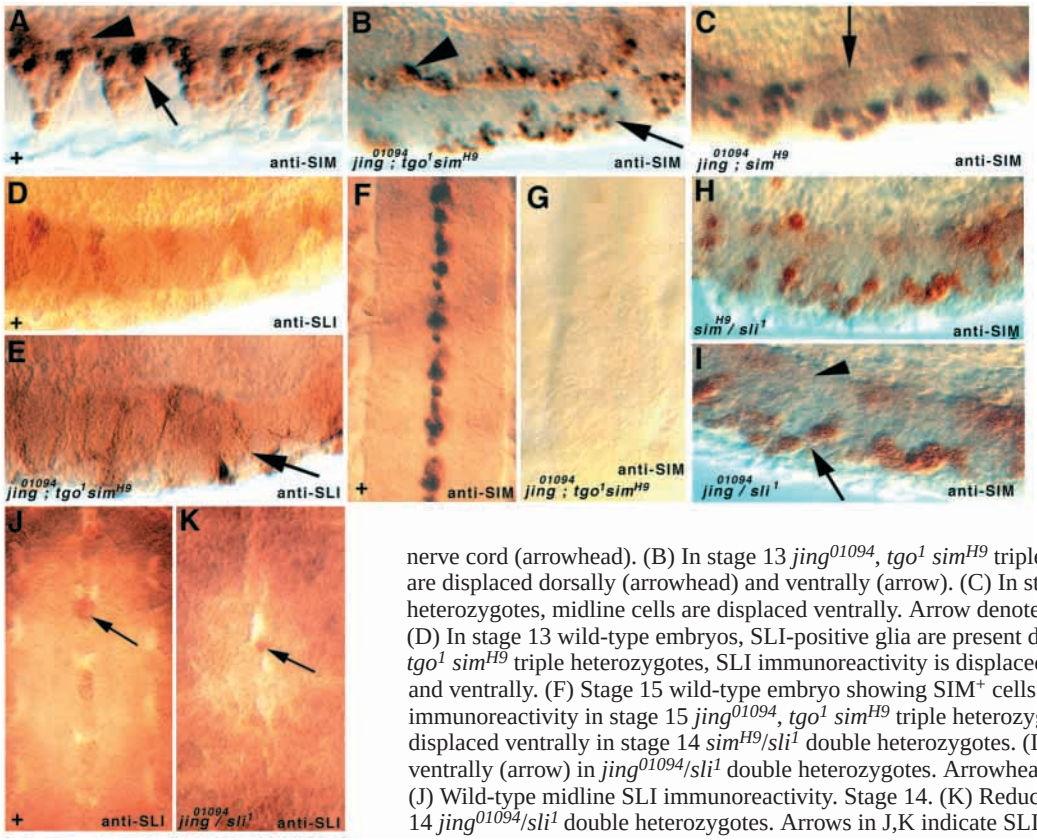

Fig. 2. Genetic interactions alter CNS midline cell development. Whole-mount embryos stained with anti-SIM (A-C,F-I) and anti-SLI (D,E,J,K). (A-E,H,I) Sagittal section with anterior towards the left and (F,G,J,K) frontal views with anterior upwards. (A) In stage 13 wild-type embryos, SIM-positive cells are distributed ventrally to dorsally (arrow) and are only occasionally outside the nerve cord (arrowhead). (B) In stage 13 *jing*^{01094}, *tgo*^{1} *sim*^{H9} triple heterozygotes, the midline cells are displaced dorsally (arrowhead) and ventrally (arrow). (C) In stage 14 *jing*^{01094}, *sim*^{H9} double heterozygotes, midline cells are displaced ventrally. Arrow denotes absence of dorsal midline cells. (D) In stage 13 wild-type embryos, SLI-positive glia are present dorsally. (E) In stage 13 *jing*^{01094}, *tgo*^{1} *sim*^{H9} triple heterozygotes, SLI immunoreactivity is displaced to segment boundaries (arrow) and ventrally. (F) Stage 15 wild-type embryo showing SIM^{+} cells. (G) Absence of SIM immunoreactivity in stage 15 *jing*^{01094}, *tgo*^{1} *sim*^{H9} triple heterozygotes. (H) SIM^{+} midline cells are displaced ventrally in stage 14 *sim*^{H9}/*sli*^{1} double heterozygotes. (I) Midline cells are displaced ventrally (arrow) in *jing*^{01094}/*sli*^{1} double heterozygotes. Arrowhead denotes absence of cells. (J) Wild-type midline SLI immunoreactivity. Stage 14. (K) Reduced SLI immunoreactivity in stage 14 *jing*^{01094}/*sli*^{1} double heterozygotes. Arrows in J,K indicate SLI immunoreactivity.

Molecular and genetic analysis of the *jing* locus

The *jing* locus encodes a transcription factor with homology to the mouse transcription factor AEBP2 (Lui and Montell, 2001). *jing*-coding sequence corresponding to the expressed sequence tag (EST) LD36562 rescues *jing* mutant effects in the ovary, confirming the identity of this gene (Lui and Montell, 2001). Fig. 4A shows the proximity of embryonic lethal *jing* P element insertions to a transcription unit (LD10015) adjacent to the *jing* 5′ regulatory region. Given the proximity of the *jing* P elements to the LD10015 transcription unit, it was important to determine whether the latter was affected by these insertions. We therefore performed in situ hybridization on embryos homozygous for *jing* P element insertional mutations (*jing*^{01094} and *jing*^{K03404}) using digoxigenin-labeled LD10015 EST as a probe. LD10015 mRNA was detected in embryos homozygous for either *jing*^{01094}or *jing*^{K03404} and therefore we conclude that LD10015 transcription is unaffected by lethal *jing* P element insertions (data not shown).

Analysis of genomic DNA sequence (GenBank Accession Number, AF285778) surrounding two lethal P-element insertions in *jing* reveals that there are three putative DNA binding sites for Tgo::Sim and Tgo::Trh (CMEs), and one for the HMG SOX protein called Fish-hook (also known as Dichaete, D – FlyBase) (TACAAT) in the 5′ regulatory region of *jing* (Fig. 4A) (Ma et al., 2000; Oshiro and Saigo, 1997; Sonnenfeld et al., 1997; Wharton et al., 1994). This raises the possibility that *jing* may be a direct transcriptional target of bHLH-PAS heterodimers and SOX proteins including TGO:SIM, TGO:TRH or Fish-hook (Crews, 1998; Ma et al., 2000).

Point mutations in *jing* were isolated by a chemical mutagenesis. From a screen of 6344 EMS-mutagenized second chromosomes, three novel *jing* mutations were isolated for failure to complement the embryonic lethality of *jing*^{K03404} genetically, therefore defining a single complementation group. *jing* EMS-induced mutations are homozygous embryonic lethal and are lethal in *trans* to *jing* P element-induced mutations and a deficiency Df(2R)ST1 covering the *jing* locus (Liu and Montell, 2001). Based on phenotypic analysis of the CNS and trachea, the *jing* EMS-induced alleles were placed in the following allelic series of phenotypic severity: *jing*^{3}>*jing*^{2}>*jing*^{1}. Molecular analysis of *jing*^{3} reveals a single nucleotide change in the coding region of this gene, confirming the identity of this complementation group (Fig. 4B). The *jing*^{3} mutation results in the conversion of tryptophan^{1200} (w^{1200}) to a premature stop codon located in the middle of the second zinc-finger motif (Fig. 4B). Given the importance of the zinc-finger motifs and a nuclear localization signal to DNA binding, the molecular nature of the *jing*^{3} mutation is consistent with its strong loss-of-function and hemizygous phenotypes. The phenotype of *jing*^{3} mutant embryos is therefore shown in phenotypic analyses.

jing embryonic expression

The expression pattern of *jing* was studied throughout embryogenesis with a *jing-lacZ* enhancer trap line (*jing*^{01094}), digoxigenin-labeled *jing* DNA probes and a rat JING antibody. *jing* mRNA and protein product are first detected during precellular blastoderm stages, suggesting that *Drosophila* embryos contain a maternal supply of *jing* (data not shown). A

discernable *jing* expression pattern is apparent from stage 9, as *jing* transcripts and protein accumulate in the CNS midline, neuroectoderm and trachea (Fig. 4C-E).

In the wild-type stage 9 CNS, *jing* mRNA is distributed in a dorsoventral pattern that is not continuous between segments (Fig. 4C). To determine the identity of the *jing*-expressing CNS cells, co-localization studies were performed using a *jing-lacZ* enhancer trap and confocal microscopy. Embryos carrying the *jing-lacZ* enhancer trap and stained with anti-β-gal and anti-SIM show co-localization in subsets of CNS midline cells during stage 9 (Fig. 4D, arrow). As SIM localizes only to midline cells in the CNS, this result confirms the midline expression of *jing* (Crews, 1998). During stage 9, *jing* transcription also occurs in the neuroectoderm and in the supraoesophageal ganglion (Fig. 4C,D).

During stage 10, JING protein is present in the tracheal placodes (Fig. 4F). A pair of JING-positive cells flank the tracheal placodes dorsally (Fig. 4F). The *jing-lacZ* enhancer trap is also expressed in TRH-positive tracheal cells in the anterior of each placode (Fig. 4G). The *jing-lacZ* enhancer trap is co-expressed with *trh* and *tgo* from stage 10 until stage 16 of embryogenesis (data not shown). JING protein is detected in all tracheal branches throughout embryonic tracheal development, consistent with a role for *jing* throughout tracheal tubulogenesis (Fig. 4H).

During stage 12/3, *jing* transcripts and protein product are present in CNS midline cells and segmental ectodermal stripes (Fig. 4I-K). By stage 14, *jing* is strongly expressed in midline glia that occupy a characteristic dorsal position in the ventral nerve cord (Fig. 4L,M). Weaker *jing* expression is detected in ventrally positioned midline neurons (Fig. 4L, black arrowhead). To determine the subcellular localization of JING in the CNS, wild-type embryos were stained with anti-JING and analyzed by confocal microscopy. By this method, JING protein can be detected within the nuclei of the midline glia (Fig. 4N, arrow) and to a lesser degree in midline neurons (Fig. 4N, arrowhead). JING protein is not detectable by confocal microscopy in cells of the lateral neuroectoderm, as opposed to *jing-lacZ* expression (see Fig. 5A) (data not shown).

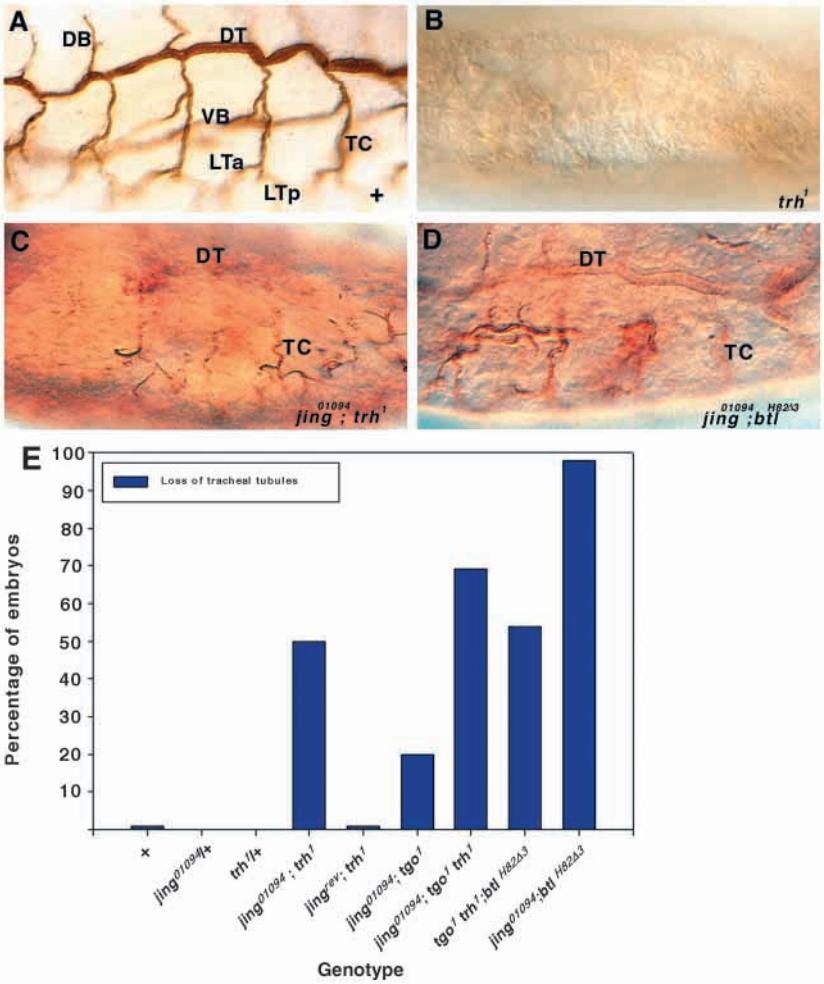

Fig. 3. Genetic interactions in the trachea. Stage 15 embryos stained with mAb 2A12 to visualize tracheal tubules and shown with anterior left in sagittal view. (A) Wild-type embryo. (B) Absence of tracheal tubules in homozygous trh^{1} mutants. (C) Severe loss of tracheal tubules in *jing* ^{01094}; trh^{1} double heterozygotes. (D) Reductions in tracheal branches in *jing* ^{01094}; $btl^{H82\Delta3}$ double heterozygotes. (E) Quantification of *jing* genetic interactions in the trachea. Double and triple heterozygous combinations (genotype). Data show the percentage of embryos with loss of tracheal branches. Tracheal development in $jing^{01094}$; trh^{1} double heterozygotes is sensitive to the dose of *tgo* ($jing^{01094}$; tgo^{1} trh^{1}). $jing^{01094}$; $btl^{H82\Delta3}$ double heterozygotes show the highest percentage of embryos with tracheal tubule defects. In all cases more than 65 embryos were scored. DB, Dorsal branch; VB, visceral branch; DT, dorsal trunk; TC, transverse connective; LTa, lateral trunk anterior; LTp, lateral trunk posterior.

Midline specificity of *jing-lacZ* expression

To further analyze *jing-lacZ*, we assessed its expression in homozygous *jing* and *sim* mutants using monoclonal anti-β-gal. During stage 14, the *jing-lacZ* enhancer shows strong expression in CNS midline cells (Fig. 5A, arrow) and weaker expression in lateral CNS cells (Fig. 5A, arrowhead). In homozygous $jing^{01094}$ mutants carrying the *jing-lacZ* P element insertion, *lacZ* expression is reduced in the entire CNS suggesting that this insertion affects *jing* gene expression and that *jing* expression may be controlled by autoregulation (Fig. 5B). By contrast, in stage 15 sim^{H9} homozygotes, *jing-lacZ* enhancer expression is absent in the CNS midline (Fig. 5C, arrow) but still present in the lateral CNS (Fig. 5C, arrowhead) and other areas of embryonic *jing* expression (data not shown). This result confirms the midline identity of the *jing-lacZ*-expressing cells.

To assess the midline identity of *jing-lacZ* enhancer expression further, we determined whether *sim* activates the *jing-lacZ* enhancer by in vivo ectopic expression experiments. The ability of *sim* to induce midline gene expression ectopically has been established (Nambu et al., 1991; Wilk et al., 1996; Xiao et al., 1996; Zelzer et al., 1997). *sim* expression was targeted to the pair-rule ectodermal stripes of the *paired* (*prd*) gene using GAL4/UAS (Brand and Perrimon, 1993) and

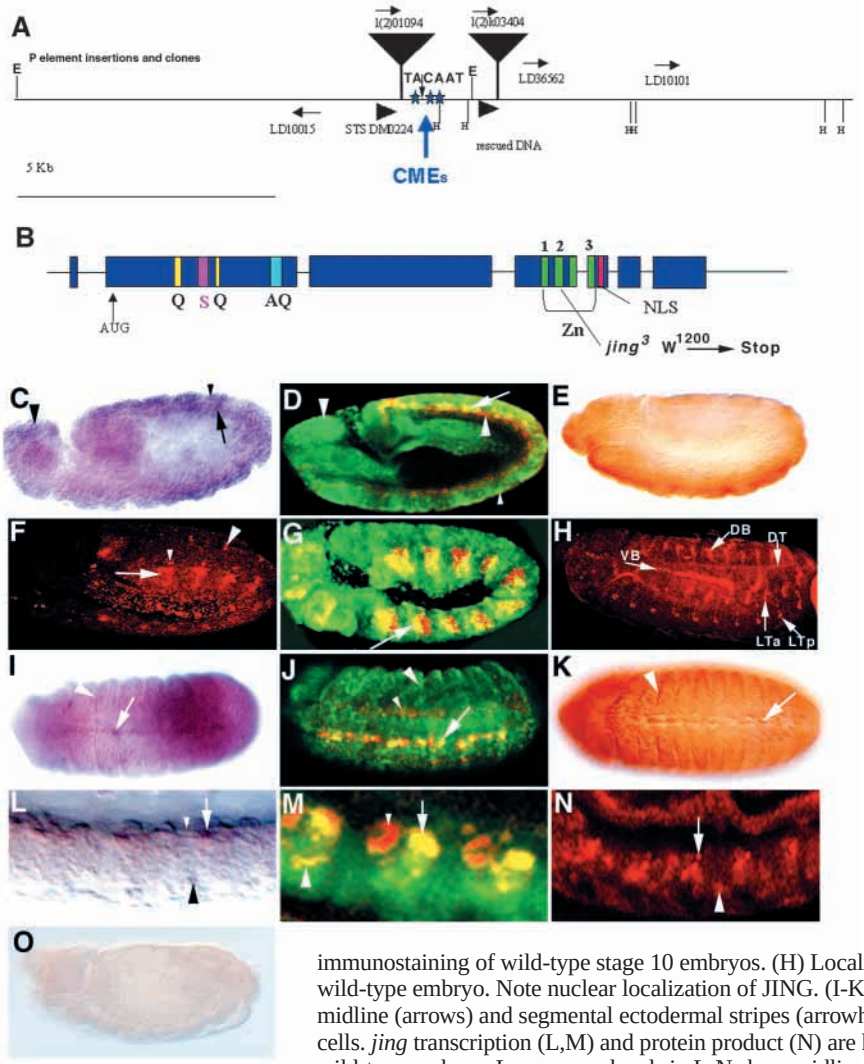

Fig. 4. *jing* genomic structure and embryonic expression. (A) Genomic interval containing *jing* ESTs, lethal P element insertions and adjacent gene (LD10015). DNA-binding sites of bHLH-PAS (CMEs) and SOX HMG protein Dichaete (TACAAT) are present in the *jing* 5′ regulatory region. (B) *jing* exon/intron structure and point mutation. Exons (filled boxes), introns (lines) and protein motifs (colored boxes). Exon 2 contains repeats of poly-glutamine (Q), poly-serine (S) and alanine-glutamine (AQ). C_2H_2-type zinc fingers (Zn). The $jing^3$ mutation is a G-to-A change at nucleotide 3806 of cDNA LD36562 converting W^{1200} to a stop codon. (C-O) Embryonic expression of *jing*. (C,I,L) In situ hybridization of *jing* digoxigenin-labeled DNA probes to wild-type embryos. (D,G,J,M) *jing-lacZ* enhancer trap expression detected via anti-β-gal staining and confocal microscopy. (E,F,H,K,N,O) Anti-JING immunostaining of wild-type embryos. Confocal microscopy (F,H,N), light microscopy (E,K,O). (C-E) By stage 9, *jing* transcripts and protein product are present in the CNS midline (arrows) and neuroectoderm (small arrowheads) and supraesophageal ganglion (arrowheads). (D) Colocalization of *jing-lacZ* product (anti-β-gal, green) and SIM (red) in a subset of CNS midline precursors at stage 9, as detected via double-label immunostaining (arrow). (F) Stage 10 embryo showing JING localization in tracheal placodes (arrow) and two adjacent cells (small arrowhead). In this focal plane, JING is observed in three MP neurons in the CNS (larger arrowhead). (G) Merged confocal image showing co-localization of *jing-lacZ* product (anti-β-gal, green) and TRH (red) in tracheal placodes (arrow) detected via double-label immunostaining of wild-type stage 10 embryos. (H) Localization of JING to all tracheal branches in a stage 15 wild-type embryo. Note nuclear localization of JING. (I-K) At stage 12/3, *jing* transcription occurs in the CNS midline (arrows) and segmental ectodermal stripes (arrowheads). Small arrowhead in J indicates Sim^+ muscle cells. *jing* transcription (L,M) and protein product (N) are highest in midline glia (arrows), as shown in a stage 15 wild-type embryo. Large arrowheads in L-N show midline neurons; small arrowheads in L,M show *jing*-negative midline glia. (O) anti-JING immunostaining of homozygous embryos carrying a deletion in the *jing* gene (Df(2R)ST1) to reveal the specificity of the antisera.

by crossing flies containing the P[*prd*-GAL4] driver, and heterozygous for the *jing-lacZ* enhancer, with flies containing P[UAS-*sim*] (Ward et al., 1998). The progeny were stained with anti-SIM to confirm ectopic expression (Fig. 5D) and with anti-β-gal to identify ectopic *jing-lacZ* expression (Fig. 5E). Ectopic expression of *sim* is sufficient to activate *jing-lacZ* in ventrally positioned cells in pair-rule ectodermal stripes (Fig. 5E,F, arrows). The ventral activation of *jing-lacZ* by *sim* is consistent with previous results showing the activation of midline-specific genes by ectopic *sim* expression (Xiao et al., 1996). In summary, the results shown here provide strong evidence that *jing* expression occurs in CNS midline cells.

jing loss- and gain-of-function disrupts CNS axon and tracheal tubule development

The *jing* expression pattern and gene dose effects in the CNS midline and trachea suggest that *jing* function may be important for the development of both systems. Therefore, CNS axon and tracheal tubule development was assessed in *jing* homozygous mutant embryos stained with monoclonal antibodies BP102 and 2A12, respectively. In $jing^3$ homozygous mutant embryos, commissural growth cones are often absent in the midline at stage 12 when compared with wild type (Fig. 6A,B). By stage 14, homozygous $jing^3$ mutants show losses of longitudinal connections and reduced commissures compared with wild type (Fig. 6C,D). Embryos double mutant for *jing* and *sim* display phenotypes similar to those of *sim* homozygotes (Fig. 6E). Therefore, the *sim* embryonic CNS axon phenotype is epistatic to that of *jing*, implying that *jing* functions downstream of *sim* (Avery and Wasserman, 1992).

The GAL4/UAS system was used to determine the effects of overexpressing *jing* in the CNS midline (Brand and Perrimon, 1993). Flies containing P[*sim*-GAL4] were crossed to flies containing P[*jing*-UAS] and their progeny stained with BP102 to assess CNS axon formation. Expression of one copy of P[*jing*-UAS] specifically in the CNS midline is sufficient to inhibit commissural and longitudinal axon formation (Fig. 6F). Therefore, the *jing* midline overexpression phenotype is similar to that resulting from *jing* loss of function (Fig. 6D), and phenotypes of *jing* and *sim* double heterozygotes (Fig. 1C). These results demonstrate that appropriate *jing* dose is a requirement for proper CNS axon development in the CNS

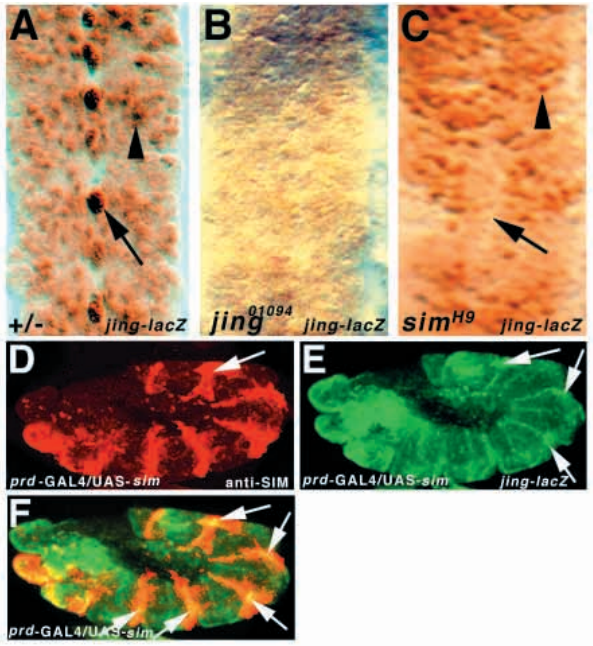

Fig. 5. The *jing-lacZ* enhancer is expressed in the midline. *lacZ* expression in whole-mount embryos heterozygous for the *jing-lacZ* enhancer trap and stained with anti-β-gal. (A) Strong midline *jing-lacZ* expression (arrow) and weaker neuroectodermal expression in stage 14 $jing^{01094}$ heterozygotes (arrowhead). (B) Reduced *jing-lacZ* expression in the midline and neuroectoderm of $jing^{01094}$ homozygotes suggests autoregulation. (C) In sim^{H9}/sim^{H9} null mutants, *jing-lacZ* midline expression is not detectable (arrow) but *lacZ* expression still occurs in the neuroectoderm (arrowhead). (D-F) Embryos heterozygous for the *jing-lacZ* enhancer trap, P[*prd*-Gal4] and P[UAS-*sim*] and stained with anti-SIM (D, red), anti-β-gal (E, green). (E) Ectopic *jing-lacZ* activation (arrows). (F) Merged images of D,E. (F) Activation of *jing-lacZ* in the ventral region of *prd* pair-rule stripes (arrows).

midline. Interestingly, we observe a similar CNS axon phenotype after overexpression of *sim* in the CNS midline (data not shown).

The homozygous *jing* CNS phenotype suggests an alteration in the mechanisms that guide CNS axons. Fasciclin 2 staining using 1D4 mAb, shows that longitudinal fascicles stall within segment boundaries causing breaks in the longitudinal tracts in 95% of $jing^3$ mutant segments (Fig. 6H, arrowhead; n=210 segments) (Van Vactor et al., 1993). A subset of normally ipsilateral axons of the most medial fascicle project instead contralaterally in $jing^3$ mutants (Fig. 6H, arrows; n=210 segments). As ipsilateral fascicles are prevented from crossing the midline in wild-type embryos (Fig. 6G), these results suggest that midline repulsive mechanisms are perturbed in *jing* mutant embryos (Hummel et al., 1999b; Kidd et al., 1999).

We next wanted to determine whether *jing* is involved in tracheal patterning due to its expression pattern and its dose-

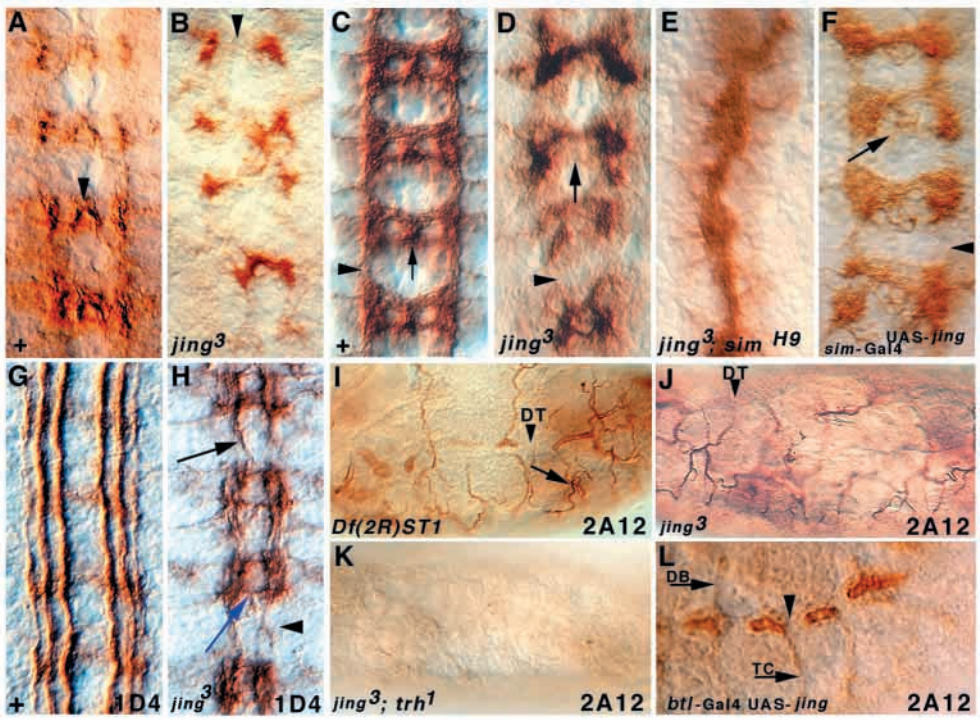

Fig. 6. *jing* loss- and gain-of-function phenotypes in the CNS and trachea. Frontal views showing CNS axon scaffolds (BP102 stain) (A-F) and longitudinal fascicles (mAb 1D4 stain; anti-Fasciclin 2) (G,H). Sagittal views of stage 15 whole-mount embryos stained with mAb 2A12 to visualize tracheal tubules (I-L). (A,B) Pioneering growth cones do not approach the midline during stage 12 in homozygous $jing^3$ mutants (B) as they do in wild-type (A) (arrowheads). (C,D) In stage 14 $jing^3$ mutants, there are variable absences of either anterior or posterior commissures (arrow) and longitudinal connectives (arrowhead) (D) compared with wild type (C). (E) $jing^3$;sim^{H9} double mutants show collapsed axon phenotypes. (F) Overexpression of *jing* in the CNS midline (*sim*-GAL4/*jing*-UAS) disrupts commissural (arrow) and longitudinal axon formation (arrowhead). (G) Ipsilateral projection of wild-type Fasciclin 2-positive longitudinal bundles. (H) In $jing^3$ homozygotes, longitudinal fascicles inappropriately cross the midline (arrows). Longitudinal fascicles stall within segments (arrowhead). (I,J) Embryos homozygous for a deficiency covering *jing* (Df(2R)ST1) and $jing^3$ mutations show defects in the formation of all tracheal branches, including the dorsal trunk (arrowhead) and transverse connectives (TC) (arrow). Note absence of the visceral branch (compare with Fig. 3A). (K) $jing^3$; trh^1 double mutants show loss of all tracheal tubules. (L) Overexpression of *jing* in the trachea (*btl*-GAL4/*jing*-UAS) disrupts all aspects of tracheal tubule development. Branch fusion in the dorsal trunk does not occur (arrowhead) and the dorsal branch and transverse connectives are reduced (arrows). The visceral branch is absent. DB, Dorsal branch; VB, visceral branch; DT, dorsal trunk; TC, transverse connective; LTa, lateral trunk anterior; LTp, lateral trunk posterior.

sensitive effects with mutations in genes controlling tracheal development. Embryos homozygous for a *jing* deficiency (Df(2R)ST1) and *jing*^{3} mutations are associated with losses of the dorsal trunk, severely disrupted transverse connectives and absences of the visceral branch (Fig. 6I,J) compared with wild-type (see Fig. 3A). Embryos doubly mutant for *jing* and *trh* lack all tracheal tubules and display phenotypes identical to *trh* homozygous mutants (Fig. 6K). Therefore, *trh* loss-of-function is epistatic to *jing* loss-of-function, implying that *jing* functions downstream of *trh*.

To determine the effects of overexpressing *jing* in the trachea, flies containing the P[*breathless* (*btl*)-GAL4] driver were crossed to those containing P[*jing*-UAS]. Progeny from this cross were stained with 2A12 antibody and tracheal tubule development was analyzed by light microscopy. Overexpression of *jing* in the trachea is associated with defects in dorsal trunk fusion, as well as improper formation of the transverse connective, dorsal branch and visceral branch (Fig. 6L). Therefore, *jing* overexpression tracheal phenotypes are similar to *jing* loss-of-function tracheal phenotypes.

jing CNS midline phenotype

Cell type-specific markers were used to follow CNS midline development in homozygous *jing* mutant embryos. Midline cells were identified using anti-SIM and the glial-specific marker anti-Slit (Nambu et al., 1990; Rothberg et al., 1990). Expression of *sli* was assessed in homozygous *jing* mutant embryos using the *lacZ* reporter P[1.0 HV, *sli-lacZ*] (Ma et al., 2000; Wharton and Crews, 1993).

There are reductions in the number of SIM-positive and *sli-lacZ* expressing midline cells in homozygous *jing*^{3} mutants compared with wild-type embryos during stage 9 and 11, respectively (Fig. 7A,B,E,F). This clearly demonstrates that the early differentiation of midline lineages requires *jing* function. By later stages of embryogenesis (stage 15), SIM and SLI immunoreactivity is drastically reduced in *jing* mutant nerve cords (Fig. 7D,H) compared with wild-type (Fig. 7C,G). The presence of SLI-positive cellular profiles in macrophages outside the VNC suggests that midline lineages are lost by cell death. Similar results were obtained using anti-Wrapper as a marker of glial identity (data not shown).

To address whether midline glia enter apoptotic pathways, *jing* mutant embryos were double-labeled with anti-SLI and TUNEL, and the occurrence of apoptotic glia monitored from stages 12 to 15 (Gavrieli et al., 1992). On average, there are one or two apoptotic midline glia within an entire nerve cord of a stage 12 wild-type embryo (Fig. 7I,I′, arrowhead; *n*=11 embryos). By contrast, every nerve cord segment in *jing*^{3} mutant embryos contains apoptotic glia in addition to the presence of more TUNEL-positive profiles in the CNS (Fig. 7J,J′; *n*=13 embryos). The increased occurrence of apoptotic glia correlates with reductions in SLI immunoreactivity in the midline of *jing*^{3} mutant embryos (Fig. 7J, arrowheads) and establishes that *jing* function is required for midline glial survival.

Enhancer traps and antibodies were used to follow the development of individual motoneurons (VUMs, 22C10) and interneurons, such as the midline precursors (MP1, dMP2, vMP2; P223, anti-ODD and 22C10) and the median neuroblast (MNB; anti-Engrailed) in wild-type and homozygous *jing*^{3} mutant embryos (Fujita et al., 1982; Hummel et al., 2000; Schmid et al., 1999; Skeath and Doe, 1998; Sonnenfeld and Jacobs, 1994; Spana et al., 1995). *jing* loss-of-function mutations are associated with reductions in the expression of all neuronal markers tested. There are absences

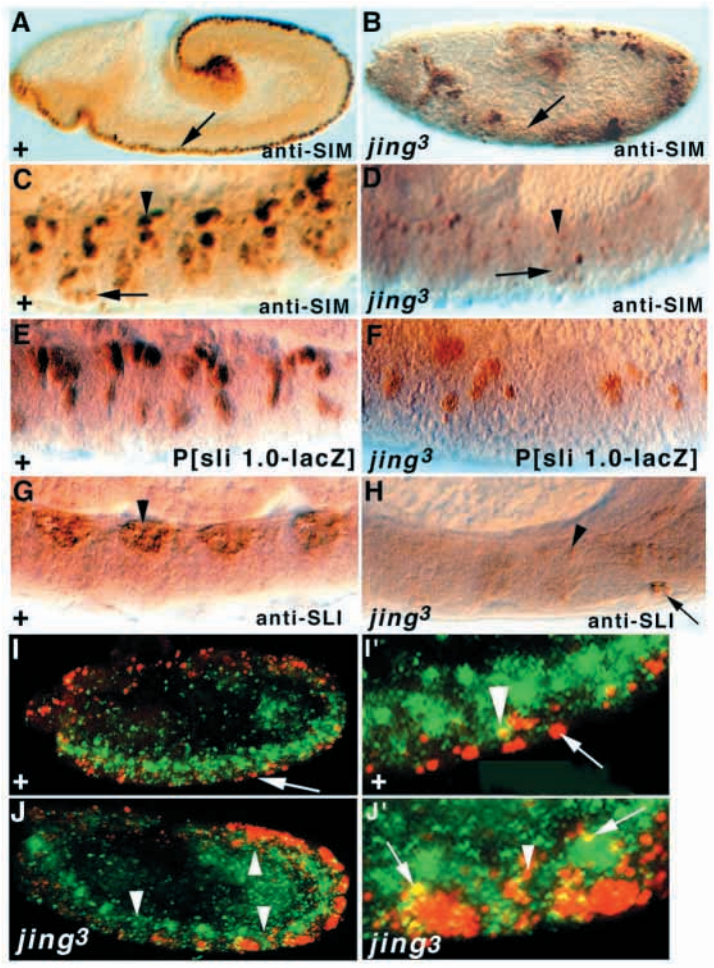

Fig. 7. *jing* mutations disrupt CNS midline glial differentiation. (A-D) Embryos stained with anti-SIM; (E,F) β-gal expression in embryos carrying *sli* reporter P[*sli* 1.0 HV-*lacZ*]; (G,H) anti-SLI stain to visualize midline glia; (I-J′) Stage 12 embryos double labeled with anti-SLI (green) and TUNEL (red), and confocal images of 1 μm serial sections. Sagittal views with anterior towards the left. (A,B) *sim* expression is reduced (arrow) in stage 9 *jing*^{3} homozygotes (B) compared with wild-type (A). (C,D) Reduced SIM immunoreactivity and small size of midline neurons (arrows) and glia (arrowheads) in stage 15 *jing*^{3} homozygotes (D) compared with wild-type (C). (E) Wild-type stage 11 expression of P[*sli* 1.0 HV-*lacZ*] in six midline glia. (F) P[*sli* 1.0 HV-*lacZ*] expression in average of 3.2 midline glia/segment in stage 11 *jing*^{3} homozygotes. (G) Wild-type SLI-positive glia during stage 15. (H) Reduced SLI immunoreactivity (arrowhead) and detection in macrophages outside the nerve cord (arrow) in stage 15 *jing*^{3} homozygotes. (I) Stage 12 wild-type *sli-lacZ* expression (green). TUNEL-positive profiles (red) are present only outside the CNS (arrow). (I′) Close-up view of I. SLI- and TUNEL-positive glia (arrowhead). (J) Loss in SLI immunoreactivity (arrowheads) in stage 12 *jing*^{3} homozygotes. Note increase in TUNEL labeling compared with wild type. (J′) Close-up view of J (arrows, dead glia). TUNEL-positive profiles in the nerve cord (arrowhead).

of immunoreactivity in the VUMs, MNB and MP1 neuronal lineages in some VNC segments in *jing*^{3} mutant embryos (Fig. 8B,D,F,H) compared with wild type (Fig. 8A,C,E,G). There is a loss of ODD immunoreactivity as early as stage 10 in MP neurons in homozygous *jing*^{3} mutants compared to wild-type (Fig. 8I,J). Similar reductions in the number of immunoreactive vMP2 and dMP2 are observed by 22C10 staining of stage10 homozygous *jing*^{3} mutant embryos (Hummel et al., 2000) (data not shown).

Within a particular VNC segment in *jing*^{3} mutants, there is a loss of Engrailed (EN)-positive neurons while the number of EN-expressing neuroectodermal cells remains equal to that in wild-type embryos (Fig. 8D, arrow). In addition, *jing* mutant embryos displaying reduced 22C10 staining of the VUMs in the CNS midline do not show any visible defects in peripheral nervous system development (data not shown). These results strongly suggest that the primary site of *jing* CNS function is at the midline.

In summary, these results demonstrate that midline neuronal and glial populations do not differentiate without proper *jing* function and suggest a positive role for *jing* in promoting CNS midline cell development.

jing tracheal phenotype

To determine the role of *jing* during tracheal development, a phenotypic analysis of homozygous *jing* mutant embryos was performed using antibodies to TRH as a marker of cell identity and to EN for identifying the anterior border of the trachea (Glazer and Shilo, 2001; Isaac and Andrew, 1996; Wilk et al., 1996). Initial defects in tracheal morphogenesis occur during tracheal placode stages in embryos homozygous mutant for all *jing* alleles (Fig. 9B). This correlates with the nuclear localization of JING in tracheal placode cells (Fig. 4). The number of TRH-positive precursors in stage 10 homozygous *jing*^{3}mutant embryos is approximately 22% of the expected number of wild-type cells (Fig. 9A,B). The relatively normal pattern of ectodermal segmentation in *jing*^{3} mutant embryos, as revealed by EN staining, suggests that the improper differentiation of tracheal cells in these mutants is not likely to result from indirect effects of ectodermal patterning (Fig. 9B,F). These results also reveal that the positioning of tracheal placodes in *jing*^{3} mutants is not altered from that of wild-type embryos.

To determine the fate of tracheal lineages we analyzed the pattern of cell death by double labeling wild-type and *jing*^{3} mutant stage 11 embryos with TUNEL and anti-TRH (Fig. 9C,D) (Gavrieli et al., 1992). Cell death is not common in the tracheal pits of wild-type stage 11 embryos (Fig. 9C). On average, there is a maximum of three TUNEL- and TRH-positive cells within an entire stage 11 wild-type embryo (n=24). By contrast, there is an average of 20 TUNEL- and TRH-positive precursors in stage 11 *jing*^{3} mutant embryos (Fig. 9D; n=34). There is also an increase in the number of apoptotic profiles surrounding the tracheal pits in *jing*^{3} compared with wild-type embryos (Fig. 9C,D, arrowhead). Cell death is observed by TUNEL labeling throughout embryogenesis in all tracheal branches in homozygous *jing*^{3} mutant embryos, suggesting that the requirement for *jing* function is not branch specific (data not shown).

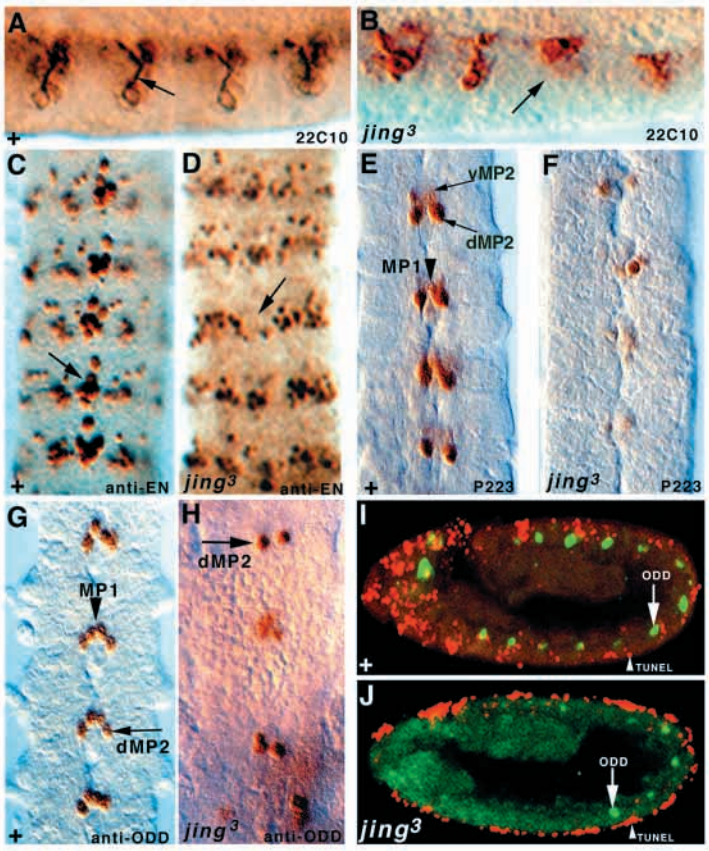

Fig. 8. *jing* mutations disrupt midline neuronal differentiation. Wild-type (A,C,E,G,I) and *jing*^{3} mutant embryos (B,D,F,H,J) stained with neuronal specific antibodies. Sagittal views of whole-mount stage 14 (A,B) and stage 10 embryos (I,J). (C-H) Frontal views of dissected stage 15 nerve cords with anterior up. (A) mAb 22C10 stains the VUM neuron cell bodies and axons projecting dorsally (arrow) in each nerve cord segment. (B) Absence of VUM cell bodies and axons in some *jing*^{3} segments (arrow). (C) Six wild-type Engrailed (EN)-positive neurons (detecting the VUMs and MNB). (D) Absence of EN-positive neurons in the CNS midline of some *jing*^{3} segments (arrow) and reductions in others. Neuroectodermal EN-positive neurons are not reduced from wild-type. (E,F) Wild-type P223 enhancer trap expression in the MP1, vMP2 and dMP2 neurons. (F) Downregulation of P223 expression in MP lineages of *jing*^{3} homozygotes. (G) Wild-type Odd-skipped (ODD) expression in MP1 and dMP2 neurons. (H) Reduced ODD expression in *jing*^{3} MP1 and dMP2 neurons. (I) Stage 10 embryo double-labeled with anti-ODD and TUNEL. Apoptotic MP lineages are not detectable. (J) Stage 10 *jing*^{3} homozygous mutant embryo double-labeled with anti-ODD and TUNEL. Note that ODD immunoreactivity is significantly reduced compared with wild type. TUNEL-positive MP neurons are not present in this embryo.

In *jing*^{3} homozygous mutant embryos, tracheal cells invaginate but the tracheal branches do not migrate properly anteriorly across EN-positive stripes as they do in wild-type embryos (Fig. 9E,F). In addition, fewer TRH-positive cells express EN in homozygous *jing*^{3} mutant embryos compared with wild-type at stage 12 (Fig. 9E,F). By stage 15 in *jing*^{3} mutant embryos, parts of the dorsal trunk, the dorsal branch and transverse connectives are missing and correlate with a loss of cells by apoptosis (Fig. 9I; data not shown). In addition, the visceral branch does not form in *jing*^{3} mutant embryos (Fig. 9I). Therefore, the EGFR-dependent visceral and dorsal trunk

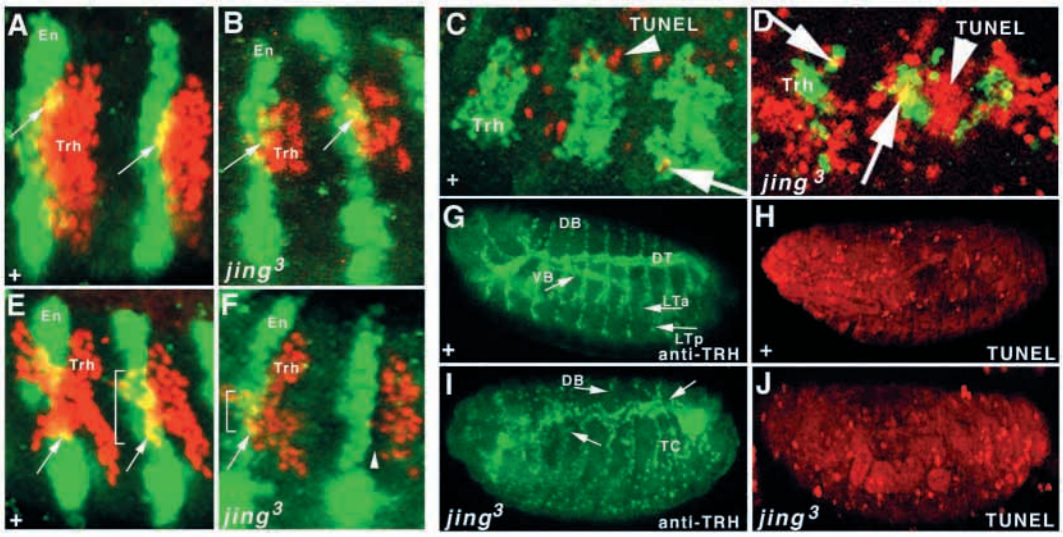

Fig. 9. *jing* tracheal phenotype. (A) Wild-type stage 10 embryo. Tracheal nuclei are visualized with anti-Trachealess (TRH, red) antibodies and anti-Engrailed (EN, green) references the anterior tracheal border. A subset of tracheal cells express EN (arrows, yellow cells). (B) In *jing*^{3} stage 10 homozygous mutant embryos, the number of TRH-positive precursors is reduced. However, the segmental EN-positive stripes and positioning of the placodes appear normal. (C) Wild-type stage 11 embryo stained with anti-TRH (green) and TUNEL (red) showing a rare apoptotic tracheal cell (arrow). (D) Stage 11 *jing*^{3} mutant embryo stained with anti-TRH (green) and TUNEL (red). Many apoptotic tracheal cells are present (arrows) and more apoptotic cells surround the pits than in wild-type embryos (arrowhead). (E) Wild-type embryo at stage 12 shows migration of primary branches across EN-positive stripes. A domain of EN-positive tracheal cells encompasses a region of the segmental stripe (bracket). (F) The domain of EN-positive migrating tracheal cells is smaller (bracket) in some stage 12 *jing*^{3} mutant segments and absent in others (arrowhead). (G,H) Wild-type stage 15 embryo stained with both anti-TRH (green, G) and TUNEL (red, H). (I,J) *jing*^{3} stage 15 homozygous mutant embryo stained with anti-TRH (green, I) and TUNEL (red, J). (I) In *jing*^{3} mutant embryos the EGFR-dependent branches are most severely affected. The visceral branch does not form and regions of the dorsal branch are absent (arrows). The number of cells in the DPP-dependent branches (DB and TC) is reduced compared with wild type. (J) By contrast, the overall apoptotic pattern in *jing*^{3} mutant embryos is not significantly elevated from wild type. DB, dorsal branch; DT, dorsal trunk; VB, visceral branch; TC, transverse connective; LTa, lateral trunk anterior; LTp, lateral trunk posterior.

branches appear more severely affected than the *Dpp*-dependent dorsal and ganglionic branches, as well as the transverse connectives in *jing*^{3}mutant embryos (Fig. 9I). Despite the death of tracheal cells in *jing* mutant embryos, the overall embryonic pattern of cell death is not significantly altered by the end of embryogenesis from that of wild-type embryos (Fig. 9H,J). Therefore, the tracheal defects in *jing* mutants are not likely to result from widespread defects in embryonic differentiation.

DISCUSSION

In this study, we provide evidence that proper functioning of the *jing* zinc-finger transcription factor is required in the CNS midline and trachea for patterning of CNS axons and tracheal tubules, respectively. The *jing* expression pattern, embryonic lethality, and loss- and gain-of-function phenotypes are consistent with an embryonic role for this locus. Given the recent characterization of *jing* during the migration of border cells in *Drosophila* ovaries, these studies highlight the important role of this gene during cellular differentiation (Lui and Montell, 2001).

Loss-of-function *jing* alleles result in aberrant expression of all CNS midline and tracheal markers tested. Loss of midline *en* expression in segments that have no detectable changes in lateral *en* expression shows that *jing* mutants have defects specific to the midline. The loss of CNS midline and tracheal cells in homozygous *jing* mutant embryos is at least partially mediated by cell death. Therefore, during embryogenesis *jing* is required for terminal differentiation and viability of CNS midline and tracheal cells.

Role of *jing* in the CNS midline

The results presented here show that CNS midline neurons and glia do not differentiate properly in homozygous *jing* mutant embryos. Several lines of evidence support this. The expression of cell-type-specific markers of midline neuronal and glial identity is altered in *jing* mutants compared with that in wild-type embryos. For example, expression of the *sli-lacZ* 1.0 HV reporter initiates in six midline glia in each wild-type nerve cord segment during stage 11 (Wharton and Crews, 1993). By contrast, *sli-lacZ* 1.0 HV reporter expression in *jing* mutants initiates in only an average of three midline glia per nerve cord segment by stage 11. In addition, there are reductions in the number of SIM-positive midline cells and ODD-positive/22C10-positive MP neurons by stage 9 in *jing*^{3} homozygous mutant embryos, respectively. Therefore, early midline glial and neuronal differentiation is aberrant in homozygous *jing* mutant embryos. By the end of embryogenesis, many neuronal and glial cell type markers are barely detectable in homozygous *jing* mutant ventral nerve cords.

The loss of *sim*, *sli*, *odd* and 22C10/*futsch* expression in *jing* mutants may reflect improper activation/regulation of gene

expression or may be secondary to cell loss. To address this issue, we analyzed the pattern of cell death in the CNS midline of *jing* mutant embryos. Apoptosis occurs in the midline glial lineage in wild-type embryos and begins during stage 12 to refine the number of cells from six to an average of three per nerve cord segment by the end of embryogenesis (Sonnenfeld and Jacobs, 1995; Zhou et al., 1995). In homozygous *jing* mutants, however, there are more apoptotic glia during stage 12 than in wild-type embryos and this correlates with the loss of SLI-positive glia. It is, therefore, likely that the loss in CNS midline gene expression in *jing* mutants results from a loss of cells. In summary, the loss in expression of cell identity markers and inappropriate cell death lead us to conclude that midline neurons and glia do not differentiate properly in *jing* mutant embryos.

The arthropod ventral nerve cord is characterized by the ladder-like pattern of the major CNS axon tracts. The nerve cord is segmental and each neuromere is connected by longitudinal axons, which are separated by anterior and posterior commissures. Disruption of this pattern by *jing* gain-of-function specifically in the CNS midline reveals the requirement for proper *jing* function within these cells for axon patterning. In addition, homozygous mutant *jing* embryos display reductions in CNS midline cells while neuroectodermal and peripheral nervous system development is unperturbed. Together, these results show that *jing* mutations have strong effects on the CNS midline and that *jing* dosage is crucial for their development.

Genetic analysis of axon patterning in the *Drosophila* CNS has revealed the important role of neuron-glial function in this process (Klämbt et al., 1991; Hummel et al., 1999b). Mutations leading to reductions in midline neuron numbers correlate with a reduction in the number of commissural tracts, whereas mutations leading to reductions in midline glia numbers show fused commissure phenotypes (Hummel et al., 1999a). These observations are consistent with the hypothesis that midline neurons (such as the VUMs) are required to attract commissural growth cones initially to the CNS midline, whereas midline glia are required subsequently for the organization of commissural axons (Hummel et al., 1999b). Based on these observations, we propose that defects in the differentiation of midline neuronal precursors, such as the VUMs, in *jing* loss-of-function mutants inhibit the attraction of commissural growth cones to the CNS midline during stage 12. As the attraction of commissural axons to the CNS midline precedes the separation of anterior from posterior commissures, the defects in midline neuronal differentiation and the associated lack of growth cones in the midline of *jing* mutants probably mask subsequent defects in glial-associated functions (Klämbt et al., 1991). During axon patterning, the MP1 interneurons participate in the formation of specific longitudinal pathways (Lin et al., 1995; Hidalgo and Brand, 1997). Therefore, the defects in MP1 neuronal differentiation in *jing* mutants may account for the inhibition in the formation of the longitudinal connectives.

Signals generated by CNS midline cells control the commissural axon pattern by either guiding growth cones toward the midline or preventing them from crossing the midline (Battye et al., 1999; Harris et al., 1996; Kidd et al., 1999; Tessier-Lavigne and Goodman, 1996). Defects in glial-associated functions occur in the CNS of homozygous *jing* mutant embryos. Reduced glial numbers and SLI production in *jing* mutants are consistent with the reduction in midline repulsion of longitudinal pathways as visualized by Fasciclin 2 staining (Fig. 6H). The remaining SLI protein product in stage 12 *jing* mutant nerve cords, however, is apparently sufficient to prevent a total collapse of the longitudinal connectives, as observed in homozygous *sim* and *sli* mutations (Nambu et al., 1990).

Role of *jing* in the trachea

This work has identified multiple roles for *jing* in tracheal morphogenesis. The earliest function of *jing* is to allocate the correct number of cells to the tracheal placodes. Several lines of evidence support this. The number of tracheal placode cells is significantly reduced from wild-type in homozygous *jing* mutant embryos. In addition, tracheal precursors die in *jing* mutant embryos, suggesting that *jing* is essential for their differentiation. As JING localizes to the nuclei of tracheal placode cells and contains potential DNA-binding and transactivation domains, it is possible that it regulates genes essential for the differentiation and survival of tracheal precursors (Mitchell and Tijian, 1989).

Although loss of *jing* function affects cellular differentiation in all tracheal lineages, it appears to have more severe effects on dorsal trunk and visceral branch development. The dorsal trunk and visceral branches derive from the same position in the tracheal placode and are induced by Epidermal Growth Factor Receptor (EGFR) (Wappner et al., 1997). EGFR is activated in the central portion of the tracheal placodes by the restricted expression of *rhomboid* (*rho*) (Bier et al., 1990; Llimargas and Casanova, 1997; Sturtevant et al., 1996; Wappner et al., 1997). The defects in dorsal trunk and visceral branch formation in homozygous *jing* mutant embryos are similar to those in embryos homozygous mutant for *Egfr* signaling (Llimargas and Casanova, 1997; Wappner et al., 1997). Given that mutations in *Egfr* pathway genes do not affect tracheal placode cell numbers, we propose that *jing* may function prior to EGFR signaling.

Several lines of evidence suggest that *jing* functions specifically in tracheal cells. First, we detect JING protein within nuclei of tracheal precursors and differentiated lineages. Second, defective placodes in *jing* mutants are observed in hemisegments with normal *en* expression patterns indicating that defects in the metamerization process do not cause the *jing* tracheal phenotype. However, we cannot rule out the possibility that Hedgehog signaling in segmental ectodermal stripes is affected by *jing* mutations. A requirement for *hh* in determining proper tracheal placode numbers in some hemisegments has recently been shown (Glazer and Shilo, 2001). Third, the most severe defects in tracheal patterning in *jing* mutant embryos occur in the dorsal trunk and visceral branch, suggesting that there is some specificity to *jing* tracheal function. Last, overexpression of *jing* specifically in the trachea results in defects in tracheal patterning that resemble *jing* loss-of-function phenotypes.

Does *jing* function in *sim*- and *trh*-dependent pathways?

Based on genetic and phenotypic analyses, we propose a role for *jing* downstream of *sim* and *trh* during CNS midline and tracheal development, respectively. First, *jing* expression is not

observed prior to that of either *sim* or *trh* in the CNS midline and trachea, respectively. *jing* expression is detected in the CNS midline during stage 9, which is after the initiation of *sim* expression and establishment of midline fates (Crews, 1998). JING protein is present in tracheal precursor nuclei, coincident with TRH during stage 10. Second, the CNS axon and tracheal phenotypes of homozygous *jing* mutations are less severe than those of homozygous *sim* and *trh* mutations, respectively. However, we cannot rule out that maternal JING may rescue the effects of zygotic *jing* mutations or that *jing* functions in a combinatorial fashion and therefore may not display severe phenotypes (Ma et al., 2000). Third, *jing* can be activated by ectopic expression of *sim*, suggesting that *sim* may regulate *jing*. The presence of three E-box ACGTG core sites in the 5′ regulatory region of *jing* suggest that this regulation may be direct. Fourth, the *sim* and *trh* embryonic phenotypes are epistatic to that of *jing*, as shown by double mutant analysis. Finally, *jing* mutations genetically interact with mutations in bHLH-PAS target genes such as *sli* and *btl* (Ma et al., 2000; Oshiro and Saigo, 1997). The ventral displacement of midline cells in *jing* and *sli* double heterozygotes strongly suggests that *jing* is required for proper *sli* regulation.

jing and CCAAT-binding proteins

In *Drosophila* ovaries, *jing* is an essential downstream target of the vertebrate homolog of the basic region/leucine zipper transcription factor CCAAT enhancer-binding protein (C/EBP), which is required for border cell migration (Liu and Montell, 2001). The JING protein is most similar to the mouse protein AEBP2, which was identified by its binding to a regulatory sequence in the adipocyte *Ap2* gene. Given that C/EBP also binds this sequence, it is proposed that JING and C/EBP coordinate cell differentiation in a co-operative manner (He et al., 1999; Liu and Montell, 2001).

An interesting parallel between the ovarian and embryonic pathways involving *jing* is the activation of *btl*. *btl* is expressed in embryonic tracheal and midline glial cells, as well as border cells of the ovary, and is essential for their migration (Glazer and Shilo, 1991; Klämbt et al., 1992; Murphy et al., 1995). *btl* is a direct target of C/EBP and TRH::TGO heterodimers in vitro (Murphy et al., 1995; Oshiro and Saigo, 1997). Therefore, the strong dominant interactions between *jing* and *btl* in the embryonic trachea coupled with the role of *jing* in border cell migration implies an important link between the maternal and embryonic pathways involving *jing*. C/EBP is expressed in the embryonic trachea after *btl* expression begins (Rorth et al., 1992). Therefore, C/EBP probably does not regulate *jing* or *btl* in the trachea, as it does in border cells. Furthermore, C/EBP expression is not sufficient to cause ectopic *btl* expression and therefore, it is proposed that this transcription factor carries out the gene expression program initiated by other factors (Murphy et al., 1995). In this way, C/EBP can function in very different pathways, including fat metabolism in adipocytes, long-term memory in Aplysia neurons and cell migration in the ovarian border cells (Murphy et al., 1995). The transcriptional capabilities of *jing* have not yet been tested and therefore it is not known whether *jing* co-operates with TGO::TRH or TGO::SIM heterodimers in activation of *btl* or other targets.

Model of JING function

We propose that bHLH-PAS heterodimers may activate *jing* transcription by binding any or all of the three CNS midline elements (CMEs) present in the 5′ regulatory region of *jing* (Fig. 10). The initiation or maintenance of *jing* transcription may also require the function of additional transcription factors such as VVL in the CNS midline and trachea or Fish-hook in

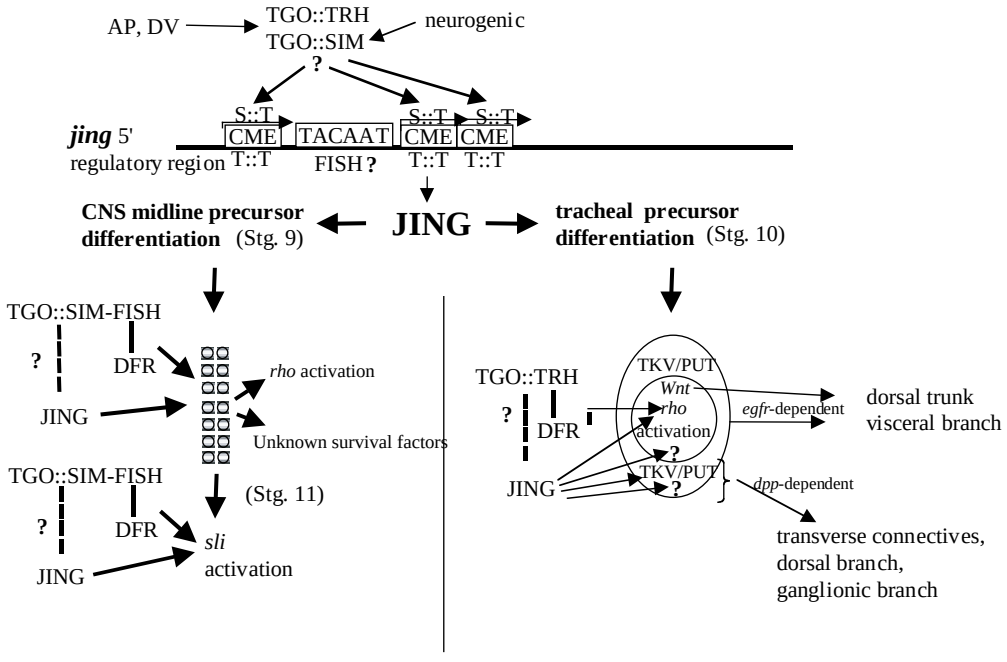

Fig. 10. Model for the role of the JING Zn-finger transcription factor in CNS midline and tracheal cell differentiation. Heterodimers of TGO:SIM and TGO:TRH may bind to the CMEs in the 5′ regulatory region of *jing*. In the CNS midline, the SOX HMG protein Dichaete (FISH in the figure) may also bind its target site, TACAAT, to promote *jing* transcription. JING enters the nucleus of CNS midline and tracheal cells where it may perform a regulatory role. This regulatory role is required for the differentiation and survival of CNS midline and tracheal precursors, possibly through the control of EGFR signaling and/or other uncharacterized survival factors. Alternatively, *jing* may function to maintain the transcriptional output initiated by bHLH-PAS, POU and SOX regulatory molecules, and failure to do so results in cell death. JING function is required throughout CNS midline and tracheal development for the formation of a functional central nervous system and tracheal tubule network. Question marks denote that direct interactions have not been demonstrated.

the CNS midline (Ma et al., 2000; Llimargas and Casanova, 1997; Boube et al., 2000; Zelzer and Shilo, 2000). The presence of a Fish-hook DNA-binding site (TACAAT) adjacent to the CMEs in the *jing* 5′ regulatory region suggests this possibility (Fig. 4A, Fig. 10).

Genetic and phenotypic evidence suggests that *jing* functions in a different manner from either *vvl* or *fish*. *vvl* and *fish* have combinatorial regulatory roles in CNS midline or tracheal pathways, and therefore *vvl* and *fish*-null embryos do not show strong phenotypes (Boube et al., 2000; Ma et al., 2000; Zelzer and Shilo, 2000). By contrast, the defects in cell numbers and increased cell death during stage 10 and 11 in *jing* mutants precede and are different from the defects in homozygous *vvl* and *dfr-fish* double mutants in the CNS midline or from *dfr* homozygotes in the trachea (Boube et al., 2000; Ma et al., 2000; Zelzer and Shilo, 2000). Therefore, activation of *jing* transcription in the CNS midline or trachea cannot be controlled exclusively by Fish-hook or VVL.

jing encodes a putative DNA-binding protein with putative transcriptional regulatory domains, and its product can be seen in the nuclei of CNS midline and tracheal cells. Based on *jing* expression patterns and phenotypes, we propose that *jing* participates in the activation of genes downstream of both SIM::TGO and TRH::TGO in the CNS midline and trachea, respectively. Whether *jing* targets are also regulated by bHLH-PAS, POU or SOX combinatorial transcriptional activities remains to be determined. Nevertheless, JING function is required to promote the differentiation of CNS midline and tracheal lineages, which, in the absence of *jing* function, do not differentiate and instead undergo apoptosis.

How does *jing* promote cellular differentiation? We propose that *jing* regulates the transcription of important survival factors including those of the EGFR pathway. For example, the *rho* gene product regulates the processing of the EGF receptor ligand Spitz and is expressed at stage 9/10 in the CNS midline and in the center region of the tracheal placodes (Bier et al., 1990; Schweitzer et al., 1995; Golembo et al., 1996; Wappner et al., 1997). Proper function of EGFR pathway genes is required for the survival of cells most highly affected by *jing* mutations, including the CNS midline glia, the tracheal dorsal trunk and visceral branches (Scholz et al., 1997; Sonnenfeld and Jacobs, 1994; Wappner et al., 1997). Furthermore, the *rho* regulatory region is controlled by TGO::TRH:DFR interactions and also contains multiple CAAT sites similar to those bound by AEBP2, the protein most related to JING (He et al., 1999; Lui and Montell, 2001; Zelzer and Shilo, 2000). This raises the possibility that *jing* may be involved in a combinatorial fashion in the regulation of bHLH-PAS target genes. However, this hypothesis does not account for the role of *jing* in EGFR-independent process such as survival of CNS midline neurons and *dpp*-dependent tracheal branches. One can then argue that *jing* function in the CNS midline and trachea is generic, and that JING carries out the gene expression programs initiated by bHLH-PAS, POU domain and SOX transcription factors. If the transcriptional programs are not maintained by *jing*, cells enter default apoptotic pathways. Alternatively, JING may be responsible for directly activating unknown survival factors in midline neurons and *dpp*-dependent tracheal branches.

We thank H. Lipshitz and Angelo Karaiskakis for help with P element-mediated transformation. We are grateful to the Ottawa General Hospital Research Institute for use of their confocal microscope. Thanks to N. Sant, C. Stefanski and C.-A. Chenard for help isolating *jing* mutations. We thank S. Crews, M. Krasnow and S. Hayashi for reagents and flies. We thank C. S. Goodman, S. Artavanis-Tsakonis and J. Skeath for antibodies. BP102, 4D9 anti-ENGRAILED/INVECTED and mAb 22C10 antibodies were obtained from the Developmental Studies Hybridoma Bank developed under the auspices of the NICHD and maintained by The University of Iowa, Department of Biological Sciences, Iowa City, IA 52242. This work was supported by a Canadian Institutes for Health Research (CIHR) operating grant to M. J. S.

REFERENCES

Adams, M. D., Celniker, S. E., Holt, R. A., Evans, C. A., Gocayne, J. D., Amanatides, P. G., Scherer, S. E., Li, P. W., Hoskins, R. A., Galle, R. F. et al. (2000). The genome sequence of *Drosophila melanogaster*. *Science* **287**, 2185-2195.

Affolter, M., Nellen, D., Nussbaumer, U. and Basler, K. (1994). Multiple requirements for the receptor serine/threonine kinase thick veins reveal novel function of TGF homologs during *Drosophila* embryogenesis. *Development* **120**, 3105-3117.

Avery, L. and Wasserman, S. (1992). Ordering gene function: the interpretation of epistasis in regulatory hierarchies. *Trends Genet.* **8**, 312-316.

Battye, R., Stevens, A. and Jacobs, J. R. (1999). Axon repulsion from the midline of the *Drosophila* CNS requires *slit* function. *Development* **126**, 2475-2481.

Bellen, H. J., O'Kane, C. J., Wilson, C., Grossniklaus, U., Pearson, R. K. and Gehring, W. J. (1989). P-element-mediated enhancer detection, a versatile method to study development in *Drosophila*. *Genes Dev.* **3**, 1288-1300.

Bier, E., Jan, L. Y. and Jan, Y. N. (1990). *rhomboid*, a gene required for dorso-ventral axis establishment and peripheral nervous system development in *Drosophila melanogaster*. *Genes Dev.* **4**, 190-203.

Booth, G. E., Kinrade, F. V. and Hidalgo, A. (2000). Glia maintain follower neuron survival during *Drosophila* CNS development. *Development* **127**, 237-244.

Bossing, T. and Technau, G. M. (1994). The fate of the CNS midline precursors in *Drosophila* as revealed by a new method for single cell labeling. *Development* **120**, 1895-1906.

Boube, M., Llimargas, M. and Casanova, J. (2000). Cross-regulatory interactions among tracheal genes support a co-operative model for the induction of tracheal fates in the *Drosophila* embryo. *Mech. Dev.* **91**, 271-278.

Brand, A. H. and Perrimon, N. (1993). Targeted gene expression as a means of altering cell fates and generating dominant phenotypes. *Development* **118**, 401-415.

Campos-Ortega, A. J. and Hartestein, V. (1985). *The Embryonic Development of* Drosophila melanogaster. New York: Springer-Verlag.

Cau, E., Gradwohl, G., Casarosa, S., Kageyama, R. and Guillemot, F. (2000). Hes genes regulate sequential stages of neurogenesis in the olfactory epithelium. *Development* **127**, 2323-2332.

Chihara, T. and Hayashi, S. (2000). Control of tracheal tubulogenesis by wingless signaling. *Development* **127**, 4433-4442.

Crews, S. T. (1998). Control of cell lineage-specific development and transcription by bHLH-PAS proteins. *Genes Dev.* **12**, 607-620.

de Celis, J. F., Llimargas, M. and Casanova, J. (1995). *ventral veinless*, the gene encoding the Cf1a transcription factor, links positional information and cell differentiation during embryonic and imaginal development in *Drosophila melanogaster*. *Development* **121**, 3405-3416.

Emmons, R. B., Duncan, D., Estes, P. A., Kiefel, P., Mosher, J. T., Sonnenfeld, M., Ward, M. P., Duncan, I. and Crews, S. T. (1999). The Spineless-Aristapedia and Tango bHLH-PAS proteins interact to control antennal and tarsal development in *Drosophila*. *Development* **126**, 3937-3945.

Estes, P., Mosher, J. and Crews, S. T. (2001). Drosophila single-minded represses gene transcription by activating the expression of repressive factors. *Dev. Biol.* **232**, 157-175.

Fujita, S. C., Zipursky, S. L., Benzer, S., Ferrus, A. and Shotwell, S. L. (1982). Monoclonal antibodies against the *Drosophila* nervous system. *Proc. Natl. Acad. Sci. USA* **79**, 7929-7933.

Gavrieli, Y., Sherman, Y. and Ben-Sasson, S. A. (1992). Identification of preprogrammed cell death in-situ via specific labeling of nuclear DNA fragmentation. *J. Cell Biol*. **119**, 493-501.

Glazer, L. and Shilo, B.-Z. (1991). The *Drosophila* FGF receptor homolog is expressed in the embryonic tracheal system and appears to be required for directed tracheal cell extension. *Genes Dev*. **5**, 697-705.

Glazer, L. and Shilo, B.-Z. (2001). Hedgehog signaling patterns the tracheal branches. *Development* **128**, 1599-1606.

Golembo, M., Raz, E. and Shilo, B.-Z. (1996). The *Drosophila* embryonic midline is the site of spitz processing and induces activation of the EGF receptor in the ventral ectoderm. *Development* **122**, 3363-3370.

Grigliatti, T. (1986). Mutagenesis. In Drosophila*: A Practical Approach* (ed. D.B. Roberts), pp. 39-58. Oxford: IRL Press Limited.

Hallam, S., Singer, E., Waring, D. and Jin, Y. (2000). The *C. elegans* NeuroD homolog *cnd-1* functions in multiple aspects of motor neuron fate specification. *Development* **127**, 4239-4252.

Harris, R., Sabatelli, L. M. and Seeger, M. A. (1996). Guidance cues at the *Drosophila* CNS midline: identification and characterization of two *Drosophila* Netrin/UNC-6 homologs. *Neuron* **17**, 217-228.

He, G. P., Kim, S. and Ro, H. S. (1999). Cloning and characterization of a novel zinc finger transcriptional repressor. A direct role of the zinc finger motif in repression. *J. Biol. Chem*. **274**, 14678-14684.

Hidalgo, A. and Brand, A. H. (1997). Targeted neuronal ablation: the role of pioneer neurons in guidance and fasciculation in the CNS of *Drosophila*. *Development* **124**, 3253-3262.

Hummel, T., Schimmelpfeng, K. and Klämbt, C. (1999a). Commissure formation in the embryonic CNS of *Drosophila*. I. Identification of the required gene functions. *Dev. Biol*. **209**, 381-398

Hummel, T., Schimmelpfeng, K. and Klämbt, C. (1999b). Commissure formation in the embryonic CNS of *Drosophila* II. Function of different midline cells. *Development* **126**, 771-779.

Hummel, T., Krukkert, K., Roos, J., Davis, G. and Klämbt, C. (2000). *Drosophila* Futsch/22C10 is a MAP1B-like protein required for dendritic and axonal development. *Neuron* **26**, 357-370.

Isaac, D. D. and Andrew, D. J. (1996). Tubulogenesis in *Drosophila*: a requirement for the *trachealess* gene product. *Genes Dev*. **10**, 103-117.

Jurata, L. W., Thomas, J. B. and Pfaff, S. L. (2000). Transcriptional mechanisms in the development of motor control. *Curr. Opin. Neurobiol*. **10**, 72-79.

Karpen, G. H. and Spradling, A. C. (1992). Analysis of subtelomeric heterochromatin in the *Drosophila* minichromosome *Dp1187* by single P element insertional mutagenesis. *Genetics* **132**, 737-753.

Kidd, T., Bland, K. and Goodman, C. S. (1999). Slit is the midline repellant for the Robo receptor in *Drosophila*. *Cell* **96**, 785-794.

Klämbt, C., Jacobs, J. R. and Goodman, C. S. (1991). The midline of the *Drosophila* central nervous system: A model for the genetic analysis of cell fate, cell migration and growth cone guidance. *Cell* **64**, 801-815.

Klämbt, C., Glazer, L. and Shilo, B.-Z. (1992). *breathless*, a *Drosophila* FGF receptor homolog, is essential for migration of tracheal and specific midline glial cells. *Genes Dev*. **6**, 1668-1678.

Lin, D. M., Fetter, R. D., Kopczynski, C., Grenningloh, G. and Goodman, C. S. (1994). Genetic analysis of fasciclin II in *Drosophila*: defasciculation, refasciculation and altered fasciculation. *Neuron* **13**, 1055-1069.

Lin, D. M., Auld, V. J. and Goodman, C. S. (1995). Targeted neuronal cell ablation in the *Drosophila* embryo: pathfinding by follower growth cones in the absence of pioneers. *Neuron* **14**, 707-715.

Liu, Y. and Montell, D. J. (2001). *jing*: a downstream target of *slbo* required for developmental control of border cell migration. *Development* **128**, 321-330.

Llimargas, M. and Casanova, J. (1997). *ventral veinless*, a POU domain transcription factor, regulates different transduction pathways required for tracheal branching in *Drosophila*. *Development* **124**, 3273-3281.

Llimargas, M. (2000). Wingless and its signaling pathway have common and separate functions during tracheal development. *Development* **127**, 4407-4417.

Ma, Y. Certel, K., Gao, Y., Niemitz, E., Mosher, J., Mukherjee, A., Mutsuddi, M., Huseinovic, N., Crews, S. T., Johnson, W. A. and Nambu, J. R. (2000). Functional interactions between *Drosophila* bHLH/PAS, Sox, and POU transcription factors regulate CNS midline expression of the slit gene. *J. Neurosci.* **20**, 4596-4605.

Mitchell, P. J. and Tijian, R. (1989). Transcriptional regulation in mammalian cells by sequence-specific DNA binding proteins. *Science* **245**, 371-378.

Moran-Rivard, L., Kagawa, T., Saueressig, H., Gross, M. K., Burrill, J. and Goulding, M. (2001). *Evx1* is a postmitotic determinant of V0 interneuron identity in the spinal cord. *Neuron* **29**, 385-399.

Morel, V. and Schweisguth, F. (2000). Repression by Suppressor of Hairless and activation by Notch are required to define a single row of *single-minded* expressing cells in the *Drosophila* embryo. *Genes Dev*. **14**, 377-388.

Murphy, A. M., Lee, T., Andrews, C. M., Shilo, B. Z. and Montell, D. J. (1995). The Breathless FGF receptor homolog, a downstream target of *Drosophila* C/EBP in the developmental control of cell migration. *Development* **121**, 2255-2263.

Nambu, J. R., Franks, R. G., Hu, S. and Crews, S. T. (1990). The *single-minded* gene of *Drosophila* is required for the expression of genes important for the development of CNS midline cells. *Cell* **63**, 63-75.

Nambu, J. R., Lewis, J. O., Wharton, K. A., Jr and Crews, S. T. (1991). The *Drosophila* single-minded gene encodes a helix-loop-helix protein that acts as a master regulator of CNS midline development. *Cell* **67**, 1-20.

Noordermeer, J. N., Kopczynski, C. C., Fetter, R. D., Bland, K. S., Chen, W. and Goodman, C. S. (1998). Wrapper, a novel member of the Ig superfamily, is expressed by midline glia and is required for them to ensheath commissural axons in *Drosophila*. *Neuron* **21**, 991-1001.

Nüsslein-Volhard, C., Wieschaus, E. and Kluding, H. (1984). Mutations affecting the larval cuticle in *Drosophila melanogaster*. I. Zygotic loci on the second chromosome. *Roux's Arch. Dev. Biol*. **193**, 267-282.

Oshiro, T. and Saigo, K. (1997). Transcriptional regulation of *breathless* FGF receptor gene by binding of TRACHEALESS/dARNT heterodimers to three central midline elements in *Drosophila* developing trachea. *Development* **124**, 3975-3986.

Patel, N. H., Schafer, B., Goodman, C. S. and Holmgren, R. (1989). The role of segment polarity genes during *Drosophila* neurogenesis. *Genes Dev.* **3**, 890-904.

Patel, N. H. (1994). Imaging neuronal subsets and other cell types in whole-mount *Drosophila* embryos and larvae using antibody probes. In Drosophila melanogaster*: Pratical Uses in Cell and Molecular Biology* (ed. E. Fyrberg and L. S. G. Goldstein), pp. 446-488. San Diego, CA: Academic Press.

Pierani, A, Moran-Rivard, L., Sunshine, M. J., Littman, D. R., Goulding, M. and Jessell, T. M. (2001). Control of interneuron fate in the developing spinal cord by the progenitor homeodomain protein Dbx1. *Neuron* **29**, 367-384.

Portman, D. S. and Emmons, S. W. (2000). The basic helix-loop-helix transcription factors LIN-32 and HLH-2 function together in mulitple steps of a *C. elegans* neuronal sublineage. *Development* **127**, 5415-5426.

Robertson, H. M., Preston, C. R., Phillis, R. W., Johnson-Schlitz, D. M., Benz, W. K. and Engels, W. R. (1988). A stable source of P-element transposase in *Drosophila melanogaster*. *Genetics* **118**, 461-470.

Rorth, P. and Montell, D. J. (1992). *Drosophila* C/EBP: a tissue-specific DNA-binding protein required for embryonic development. *Genes Dev*. **6**, 2299-2311.

Rothberg, J. M., Jacobs, J. R., Goodman, C. S. and Artavanis-Tsakonis, S. (1990). slit: an extracellular protein necessary for development of midline glia and commissural axon pathways contains both EGF and LRR domains. *Genes Dev.* **4**, 2169-2187.

Schmid, A., Chiba, A. and Doe, C. Q. (1999). Clonal analysis of *Drosophila* embryonic neuroblasts: neural cell types, axon trajectories, and muscle targets. *Development* **126**, 4653-4689.

Scholz, H., Sadlowski, E., Klaes, A. and Klämbt, C. (1997). Control of midline glia development in the embryonic *Drosophila* CNS. *Mech. Dev*. **64**, 137-151.

Schweitzer, R., Shaharabany, M., Seger, R. and Shilo, B.-Z. (1995). Secreted spitz triggers the DER signaling pathway and is a limiting component in embryonic ventral ectodermal determination. *Genes Dev*. **9**, 1518-1529.

Shiga, Y., Tanaka-Matakatsu, M. and Hayashi, S. A. (1996). Nuclear GFP/-β-galactosidase fusion protein as a marker for morphogenesis in living *Drosophila*. *Dev. Growth Differ.* **38**, 99-106.

Skeath, J. B. and Doe, C. Q. (1998). Sanpodo and Notch act in opposition to Numb to distinguish sibling *Neuron* fates in the *Drosophila* CNS. *Development* **125**, 1857-1865.

Sonnenfeld, M. J. and Jacobs, J. R. (1994). Mesectodermal cell fate analysis in *Drosophila* midline mutants. *Mech. Dev*. **46**, 3-13.

Sonnenfeld, M. J. and Jacobs, J. R. (1995). Apoptosis of the midline glia during *Drosophila* embryogenesis: a correlation with axon contact. *Development* **121**, 569-578.

Sonnenfeld, M., Ward, M., Nystrom, G., Mosher, J., Stahl, S. and Crews, S. (1997). The *Drosophila tango* gene encodes a bHLH-PAS protein that is orthologous to mammalian Arnt and controls CNS midline and tracheal development. *Development* **124**, 4583-4594.

Spana, E. P., Kopczynski, C., Goodman, C. S. and Doe, C. Q. (1995). Asymmetric localization of numb autonomously determines sibling neuron identity in the *Drosophila* CNS. *Development* **121**, 3489-3494.

Spradling, A. C. (1986). P element-mediated transformation. In Drosophila: *A Practical Approach* (ed. D. B. Roberts), pp. 175-197. Oxford-Washington DC: IRL Press.

Spradling, A. C., Stern, D., Beaton, A., Rhem, E. J., Laverty, T., Mozden, N., Misra, S. and Rubin, G. M. (1999). The Berkeley *Drosophila* Genome Project gene disruption project: Single P-element insertions mutating 25% of vital *Drosophila* genes. *Genetics* **153**, 135-177.

Sturtevant, M. A., Roark, M., O'Neill, S. W., Biehs, B., Colley, N. and Bier, E. (1996). The Drosophila rhomboid protein is concentrated in patches at the apical cell surface. *Dev. Biol.* **174**, 298-309.

Tautz, D. and Pfeifle, C. (1989). A non radioactive in situ hybridization method for the localizaton of specific RNAs in *Drosophila* embryos reveals translational control of the segmentation gene hunchback. *Chromosoma* **98**, 81-85.

Van Vactor, D., Sink, H., Fambrough, D., Tsoo, R. and Goodman, C. S. (1993). Genes that control neuromuscular specificity in *Drosophila*. *Cell* **73**, 1137-1153.

Vincent, S., Ruberte, E., Grieder, N. C., Chen, C.-K., Haerry, T., Schuh, R. and Affolter, M. (1997). DPP controls tracheal cell migration along the dorsoventral body axis of the *Drosophila* embryo. *Development* **124**, 2741-2750.

Wappner, P., Gabay, L. and Shilo, B.-Z. (1997). Interactions between the EGF receptor and Dpp pathways establish distinct cell fates in the tracheal placodes. *Development* **124**, 4707-4716.

Ward, M. P., Mosher, J. T. and Crews, S. T. (1998). Regulation of *Drosophila* bHLH-PAS protein cellular localization during embryogenesis. *Development* **125**, 1599-1608.

Wharton, K. A. and Crews, S. T. (1993). CNS midline enhancers of the *Drosophila slit* and *Toll* genes. *Mech. Dev*. **40**, 141-154.

Wharton, J. K. A., Franks, R. G., Kasai, Y. and Crews, S. T. (1994). Control of CNS midline transcription by asymmetric E-box elements: similarity to xenobiotic responsive regulation. *Development* **120**, 3563-3569.

Wilk, R., Weizman, I., Glazer, L. and Shilo, B.-Z. (1996). *trachealess* encodes a bHLH-PAS protein and is a master regulator gene in the *Drosophila* tracheal system. *Genes Dev*. **10**, 93-102.

Xiao, H., Hrdlicka, L. A. and Nambu, J. R. (1996). Alternate functions of the *single-minded* and *rhomboid* genes in development of the *Drosophila* ventral neuroectoderm. *Mech. Dev.* **58**, 65-74.

Zak, N. B., Wides, R. J., Scheijter, E. D., Raz, E. and Shilo, B.-Z. (1990). Localization of the DER/flb protein in embryos: implications on the faint little ball lethal phenotype. *Development* **109**, 865-874.

Zelzer, E. and Shilo, B.-Z. (2000). Interaction between the bHLH-PAS protein Trachealess and the POU-domain protein Drifter, specifies tracheal cell fates. *Mech. Dev.* **91**, 163-173.

Zelzer, E., Wappner, P. and Shilo, B.-Z. (1997). The PAS domain confers target gene specificity of *Drosophila* bHLH/PAS proteins. *Genes Dev*. **11**, 2079-2089.

Zhou, L., Xiao, H. and Nambu, J. R. (1997). CNS midline to mesoderm signaling in Drosophila. *Mech. Dev.* **67**, 59-68.